

AD-A189 071

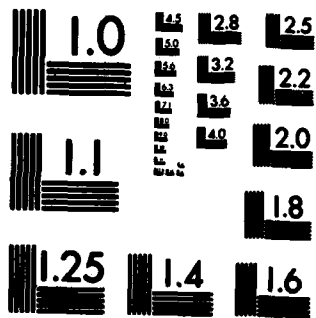
INFRARED ABSORPTION BY MOLECULAR CLUSTERS IN WATER  
VAPOR(U) CHEMICAL RESEARCH DEVELOPMENT AND ENGINEERING  
CENTER ABERDEEN PROUING GROUND MD H R CARLON DEC 89  
CRDEC-TR-88042

1/1

UNCLASSIFIED

ML

END  
DATE  
FILMED  
3 89  
DTN



MICROCOPY RESOLUTION TEST CHART  
NATIONAL BUREAU OF STANDARDS-1963-A

4

AD-A189 071

CRDEC-TR-88042

**INFRARED ABSORPTION BY  
MOLECULAR CLUSTERS IN WATER VAPOR**

**DTIC**  
**ELECTE**  
**S D**  
FEB 19 1988

by **Hugh R. Carlon**  
**RESEARCH DIRECTORATE**

**December 1987**

**EXEMPTION STATEMENT A**  
Approved for public release;  
Distribution Unlimited

**U.S. ARMY  
RESEARCH  
LABORATORIES  
CHEMICAL COMMAND**



Approved for public release; Distribution Unlimited 88042

88 2 19 077

**Disclaimer**

The findings in this report are not to be construed as an official Department of the Army position unless so designated by other authorizing documents.

**Distribution Statement**

Approved for public release; distribution is unlimited.

REPORT DOCUMENTATION PAGE

1a. REPORT SECURITY CLASSIFICATION <b>UNCLASSIFIED</b>		1b. RESTRICTIVE MARKINGS	
2a. SECURITY CLASSIFICATION AUTHORITY		3. DISTRIBUTION/AVAILABILITY OF REPORT Approved for public release; distribution is unlimited.	
2b. DECLASSIFICATION/DOWNGRADING SCHEDULE		5. MONITORING ORGANIZATION REPORT NUMBER(S)	
4. PERFORMING ORGANIZATION REPORT NUMBER(S) <b>CRDEC-TR-88042</b>		7a. NAME OF MONITORING ORGANIZATION	
6a. NAME OF PERFORMING ORGANIZATION <b>CRDEC</b>	6b. OFFICE SYMBOL (if applicable) <b>SMOCR-RSP-P</b>	7b. ADDRESS (City, State, and ZIP Code)	
6c. ADDRESS (City, State, and ZIP Code) <b>Aberdeen Proving Ground, MD 21010-5423</b>		9. PROCUREMENT INSTRUMENT IDENTIFICATION NUMBER	
8a. NAME OF FUNDING/SPONSORING ORGANIZATION <b>CRDEC</b>	8b. OFFICE SYMBOL (if applicable) <b>SMOCR-RSP-P</b>	10. SOURCE OF FUNDING NUMBERS	
8c. ADDRESS (City, State, and ZIP Code) <b>Aberdeen Proving Ground, MD 21010-5423</b>		PROGRAM ELEMENT NO. <b>1L161101</b>	TASK NO. <b>A91A</b>
11. TITLE (Include Security Classification) <b>INFRARED ABSORPTION BY MOLECULAR CLUSTERS IN WATER VAPOR</b>			
12. PERSONAL AUTHOR(S) <b>CARLOW, Hugh R.</b>			
13a. TYPE OF REPORT <b>Technical</b>	13b. TIME COVERED FROM <b>78 Jan</b> TO <b>82 Dec</b>	14. DATE OF REPORT (Year, Month, Day) <b>1987 December</b>	15. PAGE COUNT <b>80</b>
16. SUPPLEMENTARY NOTATION <i>infrared</i>			
17. COSATI CODES		18. SUBJECT TERMS (Continue on reverse if necessary and identify by block number)	
FIELD <b>20</b>	GROUP <b>03</b>	<b>(IR) Absorption, Electrical Conductivity, Steam,</b>	
<b>07</b>	<b>03</b>	<b>(IR) Emission, Water Vapor, Ions</b> ←	
19. ABSTRACT (Continue on reverse if necessary and identify by block number)			
<p>The problem of infrared absorption by molecular clusters in water vapor has been investigated by parallel researches into four different aspects of the problem:</p> <p>(1) measurements of the infrared emission of steam and of steam-generated water vapor;</p> <p>(2) measurements of the electrical conductivity of moist air humidified by steam;</p> <p>(3) modeling of simple cluster configurations and comparison of theory with experimental data; and (4) a complete study of the thermodynamics of clustering up to the critical temperature of water. The results indicate that ions are important in the formation of ion hydrates or ion-induced, neutral water clusters, which are found in great numbers in water vapor and moist air. Populations of these clusters are present in peaked distributions, probably with mean "sizes" of about 10 molecules per cluster. They exist independently of homogeneous clusters like the water dimer, which may also be significant in atmospheric processes. Cluster populations increase as the square of partial water</p> <p>(Continued on reverse.)</p> <p><i>(keywords:)</i></p>			
20. DISTRIBUTION/AVAILABILITY OF ABSTRACT <input checked="" type="checkbox"/> UNCLASSIFIED/UNLIMITED <input type="checkbox"/> SAME AS RPT. <input type="checkbox"/> DTIC USERS		21. ABSTRACT SECURITY CLASSIFICATION <b>UNCLASSIFIED</b>	
22a. NAME OF RESPONSIBLE INDIVIDUAL <b>SANDRA J. JOHNSON</b>		22b. TELEPHONE (Include Area Code) <b>(301) 671-2914</b>	22c. OFFICE SYMBOL <b>SMOCR-SPS-T</b>

## 18. SUBJECT TERMS (Continued)

Water Clusters      Molecular Clusters  
IR Spectra

## 19. ABSTRACT (Continued)

vapor pressure, and their mean size decreases with increasing temperature, approaching unity (for hydrogen-bonded clusters) at the critical temperature of 374 °C. The clusters absorb infrared radiation (and apparently radiation at other wavelengths as well) due to modes of intermolecular or ion-molecule bonds. Their individual line spectra depend upon cluster configurations, masses and bond strengths, and the literature shows reasonable agreement between calculated and actual cluster absorption wavelengths. Clustering in liquid water is much more extensive than in the vapor, but evidence exists that hydrogen bonds in clusters are similar to those in liquid water and, hence, that liquid data can be used for some cluster calculations. The hypothetical cluster formation and infrared absorption mechanisms cannot be directly verified experimentally, but there exists impressive evidence based, in part, upon data from cloud chamber, radiometric and electrical conductivity measurements, that only certain mechanisms can explain all observations. It is concluded that anomalous absorption by water vapor, including the infrared continuum absorption, can be adequately explained by the presence of neutral or charged water clusters in the vapor phase.

PREFACE

The work described in this report was performed under Project No. 1L161101A91A, Independent Laboratory In-House Research (ILIR) and was performed between January 1978 and December 1982.

The use of trade names or manufacturers' names in this report does not constitute an official endorsement of any commercial products. This report may not be cited for purposes of advertisement.

Reproduction of this document in whole or in part is prohibited except with permission of the Commander, U.S. Army Chemical Research, Development and Engineering Center, ATTN: SMCCR-SPS-T, Aberdeen Proving Ground, Maryland 21010-5423. However, the Defense Technical Information Center and the National Technical Information Service are authorized to reproduce the document for U.S. Government purposes.

Acknowledgments

The author is indebted to a great many individual investigators who contributed their valuable time to critique many of the ideas and results discussed in this work. Of the many, a few require special mention. Dr. H. A. Gebbie, at an international meeting in 1975, rekindled the author's interest in the problem of anomalous atmospheric absorption after it had lain dormant for 4 years and invited HRC to work with him on this problem at the Appleton Laboratory in Slough, England, during the summer of 1976. Dr. James L. Kassner, Jr., Director of the Graduate Center for Cloud Physics Research of the University of Missouri at Rolla, Missouri, greatly encouraged this effort. Dr. Kassner invited the author to present a seminar on anomalous absorption at the Center in 1978, and encouraged detailed discussions with experts on his staff, especially in aspects of cloud physics bearing on this problem. Dr. S. H. Suck of Dr. Kassner's staff has been especially helpful, spending many hours in fruitful discussions with the author.



Accession For	
NTIS CRA&I	<input checked="" type="checkbox"/>
DTIC TAB	<input type="checkbox"/>
Unannounced	<input type="checkbox"/>
Justification	
By	
Distribution/	
Availability Codes	
Dist	Avail. and/or Special
A-1	



## CONTENTS

	Page
1. INTRODUCTION . . . . .	9
2. REVIEW OF THE LITERATURE . . . . .	11
2.1 The Vapor (Monomer) Explanation . . . . .	11
2.2 The Dimer Explanation . . . . .	14
2.3 The "Fine Aerosol" or Water Cluster Explanation . .	15
3. METHODOLOGY . . . . .	21
3.1 Infrared Measurements . . . . .	23
3.2 Electrical Conductivity Measurements . . . . .	26
3.3 Simple Cluster Models . . . . .	32
3.4 The Thermodynamics of Clustering . . . . .	34
4. RESULTS . . . . .	43
4.1 Infrared Measurements . . . . .	43
4.2 Electrical Conductivity Measurements . . . . .	52
4.3 Simple Cluster Models . . . . .	56
4.4 The Thermodynamics of Clustering . . . . .	60
5. DISCUSSION . . . . .	63
6. SUMMARY AND CONCLUSIONS . . . . .	70
6.1 Summary . . . . .	70
6.2 Conclusions . . . . .	71
6.3 Suggestions for Future Work . . . . .	72
LITERATURE CITED . . . . .	75

LIST OF FIGURES

	Page
1. A Water Monomer . . . . .	9
2. Hydrated Ions . . . . .	10
3. The Neutral or "Homogeneous" Dimer . . . . .	11
4. Infrared Transmittance of Water Vapor . . . . .	12
5. Infrared Transmittance of Liquid Water . . . . .	16
6. Vapor-Pressure Equilibria for Clusters and Water Droplets . . . . .	19
7. Steam Test Chamber, Vertical Section . . . . .	23
8. Time-Temperature History of Typical Steam Trial; $C_D$ = Droplet Mass (Volume) Concentration, g/m <sup>3</sup> . . . . .	26
9. Simple Oscillator Model . . . . .	32
10. Absorption Coefficient Spectrum for Liquid Water . . . . .	35
11. Infrared Continuum Absorption Coefficient, 8-13 $\mu$ m . . . . .	36
12. Infrared Continuum Absorption Coefficient, 8-28 $\mu$ m . . . . .	36
13. Fraction of Water Molecules Clustered in Liquid Water and in Water Vapor . . . . .	39
14. Latent Heat of Vaporization, $\Delta H$ , vs. Weight Fraction of "O-H" in Molecule; Pure Liquid Water Corresponds to $(n_c)_L = 1.0$ . . . . .	40
15. Distribution of $Pb+(H_2O)_c$ Clusters Measured by Castleman and Tang . . . . .	40
16. Calculated Curves from Equation 29 for $k = 1.0$ and $K = 10$ . . . . .	42
17. Numbers of Water Species Per cm <sup>3</sup> ( $N_{cc}$ ) vs. Temperature for $s = 1.0$ . . . . .	43
18. Curves Computed From the Mie Theory for Water Droplet Clouds, Showing Total Extinction Coefficient (Solid Curve) with Absorption (Dashed Curve) and Scattering (Dotted Curve) Contributions, as Functions of Droplet Diameter; Wavelength = 10 $\mu$ m . . . . .	45
19. Emissivity Spectrum, Opaque Cloud Cooling From 39.0 to 31.5 °C, 28 Observations . . . . .	46
20. Emissivity Spectra, Cloud Cooling From 30.5 to 29.4 °C, 71 Observations . . . . .	47
21. Emissivity Spectrum of Figure 19 Compared to Spectrum for Opaque Cloud at 52.0 °C, 18 Observations . . . . .	48
22. Emissivity Spectrum of Upper Curve, Figure 20, Compared to Spectrum of Cooling Cloud at 56 °C, 18 Observations . . . . .	49
23. Emissivity Spectrum, Middle Curve Figure 20, Compared to Spectrum of Cooling Cloud at 52 °C, 18 Observations . . . . .	50
24. Emissivity Spectrum, Lower Curve Figure 20, Compared to Spectrum of Cooling Cloud at 52 °C, 14 Observations . . . . .	51

	Page
25. Cell Resistance vs. Humidification by Steam Generated Water Vapor. The Dashed Curve Shows Insulator Leakage Resistance for Either Cell (Representing Ions on the Insulators), and the Solid Curve, by Difference, Shows the Resistance Due Only to Moist Air Between the Large Cell Plates (Representing Ions In the Moist Air) . . . . .	53
26. N, Number of Ions Per cm <sup>3</sup> of Moist Air vs. "s", the Saturation Ratio or Fractional Relative Humidity; Celsius Air Temperatures Are Shown for Most Experimental Points . . . . .	54
27. Spectrum of Superheated Steam (400 K) Obtained by Varanasi et al. . . . .	57
28. Distributions Showing Calculated Mass Fractions of Total Water Vapor Which Are Bound into Clusters of Each Size (c) at 23 °C . . . . .	59
29. Cluster Number Distribution. $\lambda_c$ Is also Shown, from Equation 31 for $n = c$ . . . . .	60
30. Number Distribution of Homogeneous Clusters . . . . .	60
31. Variation of the Continuum Absorption Coefficient with Temperature . . . . .	62
32. Ration of Molecular Absorption Coefficients for Liquid Water and Water Vapor vs. Wavelength . . . . .	68
33. Schematic Representation of Possible Changes, with Altitude, in Water Cluster Concentration ( $C_c$ ) and Fraction of Vapor Clustered ( $(n_c)_v$ , if the Extent of Clustering Were to Increase with Altitude Due to Cosmic Radiation . . . . .	69



## INFRARED ABSORPTION BY MOLECULAR CLUSTERS IN WATER VAPOR

### 1. INTRODUCTION

It is customary to think of water vapor as a gas, consisting entirely of individual water molecules, or "monomers". The hydrogen (H) and oxygen (O) atoms in a single water molecule, or monomer, are shown schematically in Figure 1.

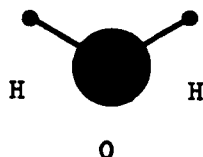


Figure 1. A Water Monomer.

In water vapor, huge numbers of monomers are randomly oriented. For example, at 20 °C, about  $10^{18}$  monomers can be found in each  $\text{cm}^3$  of atmospheric air at sea level.

For many years it was believed that the infrared spectrum of water, like the spectra of most gases, could be modeled using theoretical band models or line shapes. But as instrumentation became more sophisticated, it became apparent that the infrared absorption of water vapor has unusual pressure and temperature dependencies. Spectroscopists attempted to explain the discrepancies, which manifested themselves as "anomalous" or excessive absorption compared to that expected from theory, as being due to absorption of the far wings of known interatomic vibrational or rotation bands of the water monomer.

Explanation of the discrepancies have become increasingly suspect during the past decade. Evidence exists purporting the anomalous absorption in water vapor could be due not to interatomic or rotational modes of the monomer, but to intermolecular modes, for example, hydrogen bonds between water molecules. The bound water molecules would form groups of lattices of molecules in the vapor phase, producing "water clusters". The cluster species could be of many kinds and sizes, and would not be limited to hydrogen-bonded species. For example, water molecules could form about positive or negative ions, as shown schematically in Figure 2, forming "ion clusters" or "hydrated ions", which might add absorbing modes of their own to the infrared spectrum.

Infrared measurements, and measurements at longer (mm-wave and radar) wavelengths, about  $10^{14}$  water molecules per  $\text{cm}^3$

(20 °C), would have to be involved in clustering to explain the observed levels of anomalous absorption. The extent of clustering in water vapor at 20 °C would have to be about  $10^{14}$  divided by  $10^{18}$  monomers per  $\text{cm}^3$ , or about  $10^{-4}$ .



Figure 2. Hydrated Ions.

A cluster explanation of anomalous absorption in water vapor is attractive for many other reasons. For example, this absorption resembles the infrared absorption of liquid water, which is extensively hydrogen-bonded. Some earlier reports sought to explain anomalous absorption by the vapor as being due to traces of fine liquid water "aerosols". Clustering at the molecular or ionic levels was not yet fully appreciated when these reports appeared. Also, the cluster explanation can be shown to be consistent with the nature of water species which are known by cloud physicists and by scientists studying atmospheric electricity, to exist in moist air. There is thermodynamic consistency as well, and there are close parallels with the nucleation theory.

Despite the attractiveness of a cluster explanation of anomalous absorption by water vapor, it is still widely accepted that extensions of vapor theory can explain this phenomenon. The work discussed in this report was performed with the objective of seriously studying cluster formation in water vapor, to answer several interrelated questions which can together be taken as a statement of the problem investigated in this effort:

- How do complexes or "clusters" of water molecules form in water vapor, and how are their numbers and kinds affected by thermodynamic parameters?
- What are the mechanisms of infrared absorption by molecular clusters in water vapor, and what do their predicted infrared spectra look like?
- Can the hypothetical cluster formation and infrared absorption mechanisms be verified experimentally?
- Can anomalous infrared absorption by water vapor be explained by the presence of neutral or charged cluster species in the vapor phase?

The problem is important because anomalous infrared absorption greatly affects the radiative transfer of the atmosphere and, hence, the earth's climate, in ways which can only be understood by understanding the mechanisms which are responsible. Also, there are potentially dozens and perhaps hundreds of practical applications for new results related to this problem, if it can be successfully solved.

The study addressed in this report was limited to electrical and spectral properties of molecular clusters of water, in water vapor or in moist air, and specifically to the emission spectra of these clusters in the infrared wavelength region.

## 2. REVIEW OF THE LITERATURE

There are three possible explanations for the anomalous absorption of water vapor. The first is the vapor or monomer explanation, which seeks to relate spectral observations to classical band or line models for gases, where these models have been empirically modified. The second is the dimer explanation, which considers the electrically-neutral cluster of size two,  $(\text{H}_2\text{O})_2$ , as by far the most likely to occur in the water vapor. Thus, the dimer (Figure 3), where the dotted line represents a hydrogen bond, would produce anomalous absorption due to modes of this intermolecular (hydrogen) bond.

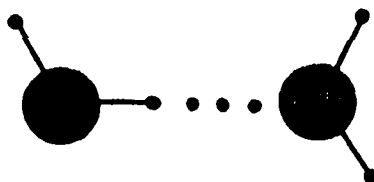


Figure 3. The Neutral or "Homogeneous" Dimer.

The third explanation is the one most extensively studied in this report. Namely, that statistical distributions of charged or neutral clusters in water vapor can account for the observed anomalous absorption, and that the dimer is but one of myriad cluster species which can exist in water vapor or in moist air. The literature pertaining to each of these explanations is reviewed in the following paragraphs.

### 2.1 The Vapor (Monomer) Explanation.

The basic concepts of vapor spectroscopy in the infrared were already known in the later 19th century. By the 1930s, many common gases or vapors had been investigated, and infrared instrumentation had become sufficiently sensitive to reveal that

water vapor behaved differently than most other gases. Elsasser<sup>1</sup> first published an empirical modification to the classical models, which attributed anomalous infrared absorption to the lower-wavelength "wing" of the water "rotational band". The infrared transmittance spectrum of water vapor is shown in Figure 4, where percent transmittance is plotted as a function of wavelength in microns or micrometers ( $\mu\text{m}$ ). Transmittance (transmission) is the reciprocal of absorbance (absorption), although the word pairs are defined somewhat differently. Anomalous infrared absorption (reduced transmission) of water vapor can be measured at wavelengths as short as 3-5  $\mu\text{m}$ .

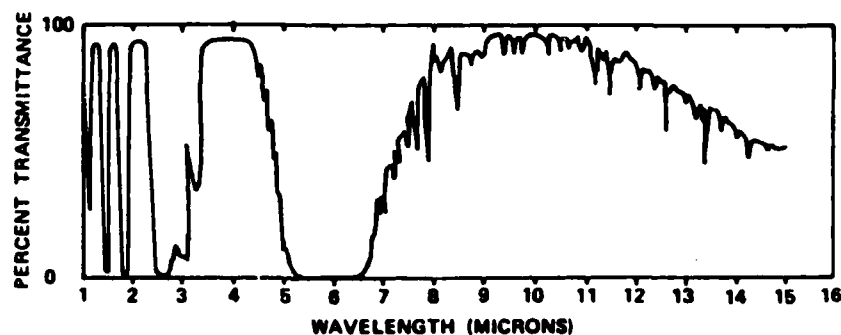


Figure 4. Infrared Transmittance of Water Vapor.

Anomalous absorption increases in strength through the wavelength region from 7  $\mu\text{m}$  to 20 or 30  $\mu\text{m}$  (the latter wavelengths are not shown in Figure 4). The "rotational band" of water vapor is a broad absorption peak extending from about 30  $\mu\text{m}$  to beyond 40  $\mu\text{m}$ . Thus, Elsasser sought to explain the anomalous absorption in the 7-15  $\mu\text{m}$  region as being due to the shorter-wavelength "wing" of this band, which is attributed to water vapor (monomers). For most applications, for example, for the operation of electro-optical systems through the atmosphere, the regions of high transparency (called "windows") shown at 3-5  $\mu\text{m}$  and 7-15  $\mu\text{m}$  in Figure 4 are of great interest. Other atmospheric gases, including  $\text{CO}_2$ , absorb at longer wavelengths. The bands at wavelengths nearer and shorter than about 3  $\mu\text{m}$  and the band centered at 6  $\mu\text{m}$  are attributable to modes of the water monomer, that is, to modes of interatomic bonds linking hydrogen and oxygen atoms, as shown schematically by the lines in Figure 1. The anomalous infrared absorption lying between bands of absorption due to interatomic modes tends to limit infrared systems performance in the 3-5  $\mu\text{m}$  and 7-15  $\mu\text{m}$  atmospheric "window" regions, and produces other important effects which will be discussed subsequently. This anomalous absorption, in the 3-5  $\mu\text{m}$  and 7-15  $\mu\text{m}$  windows, is frequently referred to as the "infrared continuum absorption".

Goody<sup>2</sup> and Smith<sup>3</sup> have republished Elsasser's hypotheses until they have become generally accepted as "theory" by vapor spectroscopists. Unfortunately, there was major, and probably incorrect, assumption in Elsasser's work. Elsasser assumed, as have many workers since him, that water vapor is the same substance regardless of the temperature at which it exists. That is, he viewed water vapor as a homogeneous gas at all vapor temperatures and pressures, and he used steam data interchangeably with lower temperature water vapor data. In fact, Elsasser's empirical model was based upon steam measurements. Elsasser stated that the anomalous or continuum absorption was not observable in water vapor at room temperature, but that it could be measured and modeled in infrared spectra of steam. In recent years, it has become known that steam contains large populations of water clusters, and that these populations increase very rapidly with increasing temperature. It is possible that Elsasser actually modeled anomalous ir absorption due to water clusters, but that he explained his observations by modifying existing vapor (monomer) theories.

Elsasser's explanation of anomalous or continuum absorption in water vapor is still widely accepted by vapor spectroscopists, and his use of empirical modifications to classical theory has been taken as license for subsequent workers to do the same. The following discussion will illustrate this point.

Line-by-line theoretical calculations of the absorption coefficient,  $\alpha(\nu)$ , of atmospheric water vapor usually are based upon a simple or modified form of the Lorentz profile,  $f(\nu)$ , as discussed by VanVleck and Weisskopf:<sup>4</sup>

$$\alpha(\nu) = S \cdot f(\nu) = S \cdot \frac{\gamma}{n[(\nu - \nu_0)^2 + \gamma^2]} \quad (1)$$

for a line centered at  $\nu_0$  and at an observation frequency  $\nu$ , where  $S$  is the integrated line strength,  $\gamma$  is the line half-width given by:

$$\gamma = \gamma_0 (P/P_0 / (T_0/T))^{1/2} \quad (2)$$

and  $\gamma_0$  is the half-width at some standard pressure ( $P_0$ ) and temperature ( $T_0$ ).

At reduced pressures, such as those found in the upper atmosphere, other profiles sometimes are used. For example, Penner<sup>5</sup> discussed the Voigt profile which may be obtained by convolving the Lorentz and Doppler profiles. On the far wings

of strong absorption bands (for example, in the infrared continuum absorption region on the lower-wavelength wing of the water vapor rotational band), considerable manipulation of the line profile is necessary to approach a fit to experimental data, at least in the case of water vapor. For example, the "super-Lorentz" shape on the far wings<sup>6,7</sup> is:

$$f(\nu) = \frac{C\gamma(\nu_m)^n}{\pi(\nu_m^2 + \gamma^2)} \left( \frac{1}{\nu - \nu_0} \right)^n \quad \text{where} \quad |(\nu - \nu_0)| \geq \nu_m \quad (3)$$

and where  $n$  and  $\nu_m$  are empirically-determined parameters and  $C$  is a normalization constant. Thus, "super-Voigt" convolutions are possible. Additional terms may be added until empirical fits to experimentally-observed spectra are obtained. But in the process, the theoretical basis of the model becomes increasingly strained so that an explanation of an empirical data fit based in theory becomes increasingly difficult to justify.

Working with superheated steam, Varanasi et al.<sup>8</sup> showed that infrared absorption in water "vapor" (steam) had a negative temperature dependency, which could be explained by traces of the water dimer or hydrogen-bonded cluster of two water molecules, in the vapor phase. A negative temperature dependency was the first solid evidence that a vapor explanation might be inadequate to describe the infrared continuum absorption.

## 2.2 The Dimer Explanation.

Varanasi's et al.<sup>8</sup> indication that the dimer (Figure 3) could be responsible for the anomalous or infrared continuum absorption of water vapor found support in the results of some preliminary investigations at other wavelengths by Burroughs et al.<sup>9</sup> Bignell<sup>10</sup> found similar results in extensive new measurements of water vapor, and he also related them to the dimer. He suggested: (1) the homogeneous water dimer  $(H_2O)_2$ , if it exists in the atmosphere, must be in very small abundance; (2) its mole fraction should vary linearly with partial water vapor pressure and should decrease by about 2% per °C with rising temperature near 300 K; and (3) its infrared spectrum should consist of very wide lines resulting in a continuumlike absorption. Penner<sup>11</sup> further discussed dimer absorption. Gebbie et al.<sup>12</sup> stated the view that anomalous absorption of the atmosphere was due largely, if not entirely, to the molecular complexity of water vapor. Emery et al.<sup>13</sup> found anomalous absorption in the sub-mm and mm-wave regions characterized by much higher binding energies than could be assigned to the equilibrium water dimer. This led to the conclusion<sup>14</sup> that anomalous absorption in the atmosphere at low temperatures cannot be attributed to water dimers in equilibrium.

Curtiss and Pople<sup>15</sup> have reported calculations of dimer bending frequencies in the 20-25  $\mu\text{m}$  wavelength range, but these have not been very helpful in explaining the infrared continuum absorption at 7-15  $\mu\text{m}$  and particularly in the 3-5  $\mu\text{m}$  region. Owicki et al.<sup>16</sup> studied dimer energetics and placed the shortest absorption wavelength near 13  $\mu\text{m}$ . The shortest absorpton wavelength is accompanied by lines extending to beyond 100  $\mu\text{m}$ , and the spectra bear little resemblance to the observed anomalous or continuum spectra.

The dimer hypothesis called the attention of vapor spectroscopists to the possibility that water vapor might not be a homogeneous gas, but might contain water clusters which could explain the continuum absorption. Thus, a cluster term is sometimes included in more recent vapor model equations. But those working most closely with the dimer hypothesis, notably Gebbie and his co-workers, have reached the conclusion that the dimer, alone, cannot account for anomalous absorption observed in many different wavelength regions.

### 2.3 The "Fine Aerosol" or Water Cluster Explanation.

The present author, working on problems of atmospheric infrared transmission, independently developed a third hypothesis to explain the infrared continuum absorption. Although this work was performed over a span of time roughly parallel to that of the dimerists, it was not until a colloquium on atmospheric constituents was held by the Inter-Union Commission on Radio-Meteorology<sup>17</sup> that this author, the dimerists, and some vapor spectroscopists became aware that each was addressing the same phenomenon. The dimerists and vapor spectroscopists addressed the anomalous absorption by atmospheric water vapor in the infrared (the "continuum" absorption) and at sub-mm, mm, and radar wavelengths.

Carlson<sup>18</sup> found evidence of anomalous infrared absorption in field measurements of turbulence. He recognized that infrared absorption, which was modulating optical beams in the 8-13  $\mu\text{m}$  wavelength region, could be caused by small concentrations of tiny liquid droplets floating in moist air. The transmittance spectrum of liquid water is shown in Figure 5, as a function of wavelength,  $\mu\text{m}$ , and of "wavenumber", the reciprocal of wavelength in cm, a unit used commonly by spectroscopists.

A comparison of Figure 5 for liquid water to Figure 4 for water vapor will show that both spectra have absorption (reduced transmittance) bands near 3  $\mu\text{m}$  and 6  $\mu\text{m}$ , due to interatomic modes of the water monomer (Figure 1). Absorption bands are found to be about equally intense in the liquid and vapor phases. Bryan and Curnutte<sup>19</sup> have given locations for several of these interatomic bands, which are shown in Table 1.

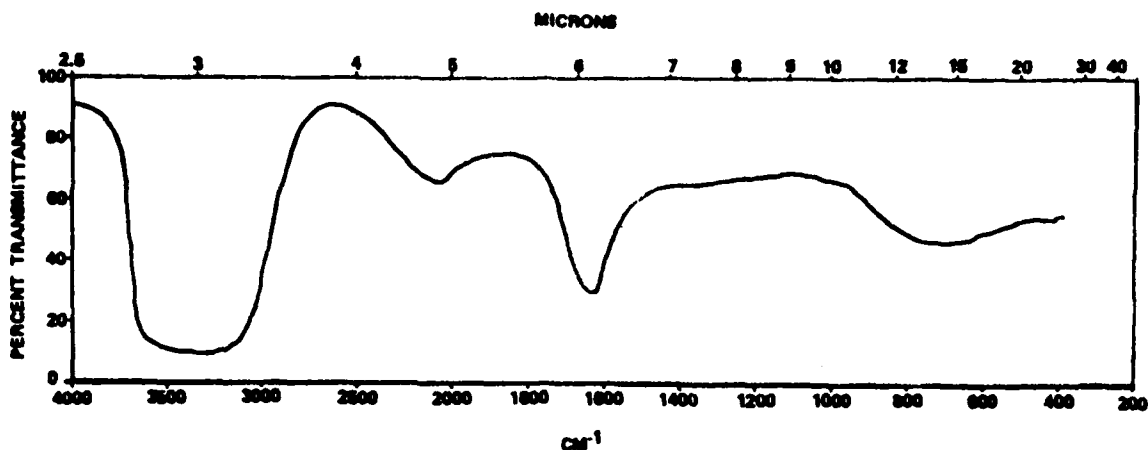


Figure 5. Infrared Transmittance of Liquid Water.

Table 1. Interatomic Band Locations for Water in the Vapor and Liquid Phases.

Band Designation	Vapor Phase		Liquid Phase	
	Wavelength (μm)	Frequency (cm <sup>-1</sup> )	Wavelength (μm)	Frequency (cm <sup>-1</sup> )
v1	2.76	3625	2.90	3450
v2	6.27	1595	6.10	1640
v3	2.66	3756	2.77	3615

Carlson observed, however, that there is a major difference between the liquid and vapor phases. In the wavelength regions between absorption bands of interatomic modes, where the infrared continuum absorption occurs, equal masses of liquid water and of water vapor have vastly different absorption levels. Carlson showed that the liquid water absorption is  $10^3 - 10^4$  greater than that of the vapor in the  $10 \mu\text{m}$  wavelength region. The enhanced liquid water absorption is due to intermolecular (hydrogen) bonds in the liquid phase. To state the same thing in another way, Carlson showed that if only  $10^{-4} - 10^{-3}$  of all water were present as tiny droplets in the vapor phase, the absorption near the  $10 \mu\text{m}$  wavelength would be as great from these droplets as from the great majority of water present as the vapor. But, because the infrared continuum absorption often was very strong in the absence of any atmospheric haze or reduced visibility due to aerosols, Carlson

realized that these hypothetical droplets must be extremely small, too small to scatter visible light.

Carlson<sup>20</sup> hypothesized that if these tiny liquid droplets or "aerosols" were present in water vapor, they could affect radiometric readings and measurements, for example from earth satellites, and might provide a means for detection of clear-air turbulence (CAT) ahead of aircraft equipped with an infrared radiometer. Subsequent work by Kuhn et al.<sup>21</sup> has shown that CAT detection is possible using such equipment. Streete<sup>22</sup> saw the possible importance of tiny aerosol droplets in explaining his atmospheric transmission data in the infrared. But confusion still existed as to how these droplets formed. If condensation nuclei were necessary, as for the formation of common fog droplets, then these nuclei or droplets should have been large enough to optically scatter and to cause haze and reduced visibility whenever anomalous infrared absorption were present.

Carlson<sup>23</sup> reported many examples of infrared phenomena, which could be explained by his "fine aerosol" hypothesis; and for the first time, he used this interpretation as possible explanation of the infrared water vapor continuum. A year later, Carlson<sup>24</sup> published measurements of infrared emission from cooling steam, which showed conclusively that tiny liquidlike species could account for major changes in radiance even through apparently clear atmospheres. Hodges<sup>25</sup> referenced this work in reporting new aerosol data. Carlson et al.<sup>26</sup> repeated the steam measurements with extensive instrumentation and found clear-cut evidence for clustering, which led to recent experiments described in later sections of this report.

By 1975, Carlson and other workers discovered that the "tiny aerosols" described by Carlson, and the dimer or other water cluster species, might in fact be the same species. The examples in Carlson's earlier reports of infrared radiometric activity due to tiny aerosols might actually be examples of atmospheric water cluster activity. This argument was furthered by droplet equilibrium considerations described by Wilson,<sup>27</sup> after whom Figure 6 has been drawn. Wilson summarized a great deal of prior work on the condensation and growth of droplets. He derived the expression for equilibrium of (charged) droplets in water vapor or in moist air:

$$\frac{R\theta_0}{M} \ln(p/p_0) = \frac{2T}{r} + \frac{dT}{dr} - \left( \frac{1}{e_1} - \frac{1}{e_2} \right) \frac{q^2}{8_{11r^4}} \quad (4)$$

where  $R$  is the gas constant =  $8.314 \times 10^7$  ergs/°K-mole,  $\theta$  is the absolute temperature, °K,  $\rho$  is the density of the droplet, g/cm<sup>3</sup>,  $M$  is the molecular weight, g,  $p/p_0$  is the equilibrium saturation (or supersaturation) ratio, also abbreviated "s" in Figure 6.  $T$  is the surface tension, dynes/m,  $r$  is the droplet radius in cm (when used with subscript, as  $r_\mu$ , denotes radius in micrometers as shown on the abscissa of Figure 6),  $\epsilon_1$  and  $\epsilon_2$  are (respectively) the dielectric constants of the vapor and of the condensed liquid, and  $q$  is the electronic charge,  $4.813 \times 10^{-10}$  statcoulomb. Assuming the surface tension is independent of droplet radius (an imprecise assumption), Equation 4 at 0 °C yields the curve labeled "ion" in Figure 6. If a tiny droplet or cluster of molecules is uncharged, the right-hand (subtractive) term of Equation 4 becomes zero, and the equilibrium curve is shown dotted in Figure 6 and labeled "uncharged". The author has also drawn dashed curves in the figure which correspond to classes of condensation nuclei found in real atmospheres and upon which water can condense to grow droplets. These classes are Aitken nuclei, combustion (continental) nuclei, and salt (maritime) nuclei, respectively, as arranged by increasing radius.

The interpretation of the equilibrium curves is as follows. Points above a given curve represent drops surrounded by vapor which will condense upon them and therefore are a domain of drop growth. Points below a curve are in the domain of evaporation. Uncharged or neutral clusters (dotted curve, Figure 6) should grow indefinitely until external factors remove the condition of supersaturation. But the "ion" curve, because of the subtractive charge term in Equation 4, has a maximum at a supersaturation  $s = 4.2$ , corresponding, according to Wilson, to ion clusters of about 30 water molecules. This is the "critical" cluster size or radius. Until the ion cluster of 30 water molecules is reached, a droplet cannot be "nucleated" to grow indefinitely into a fog-sized droplet. But, there is a portion of the "ion" curve in Figure 6 which does exist as a real equilibrium case in real atmospheres. The real equilibrium case is the near-vertical portion of the ion curve corresponding to relative humidities of or less than 100% ( $s \leq 1.0$ ). The curves show that equilibrium distributions of ion clusters (ion hydrates) are true constituents of moist atmospheres, and that the mean size of these clusters is dependent upon the saturation ratio for the moist gas. The 3 classes of condensation nuclei shown in Figure 6 also are well known to exist in real atmospheres. The curves indicate that as these nuclei are hydrated and droplets grow, the rate of growth becomes very rapid at high saturations ("s" values) approaching 1.0. Droplets grown on these nuclei should reach radii capable of scattering visible light (at least  $r_\mu = 10^{-1} \mu\text{m}$ ) before saturation humidity is attained. Therefore, these species should produce hazes and reduced visibility at high humidities.

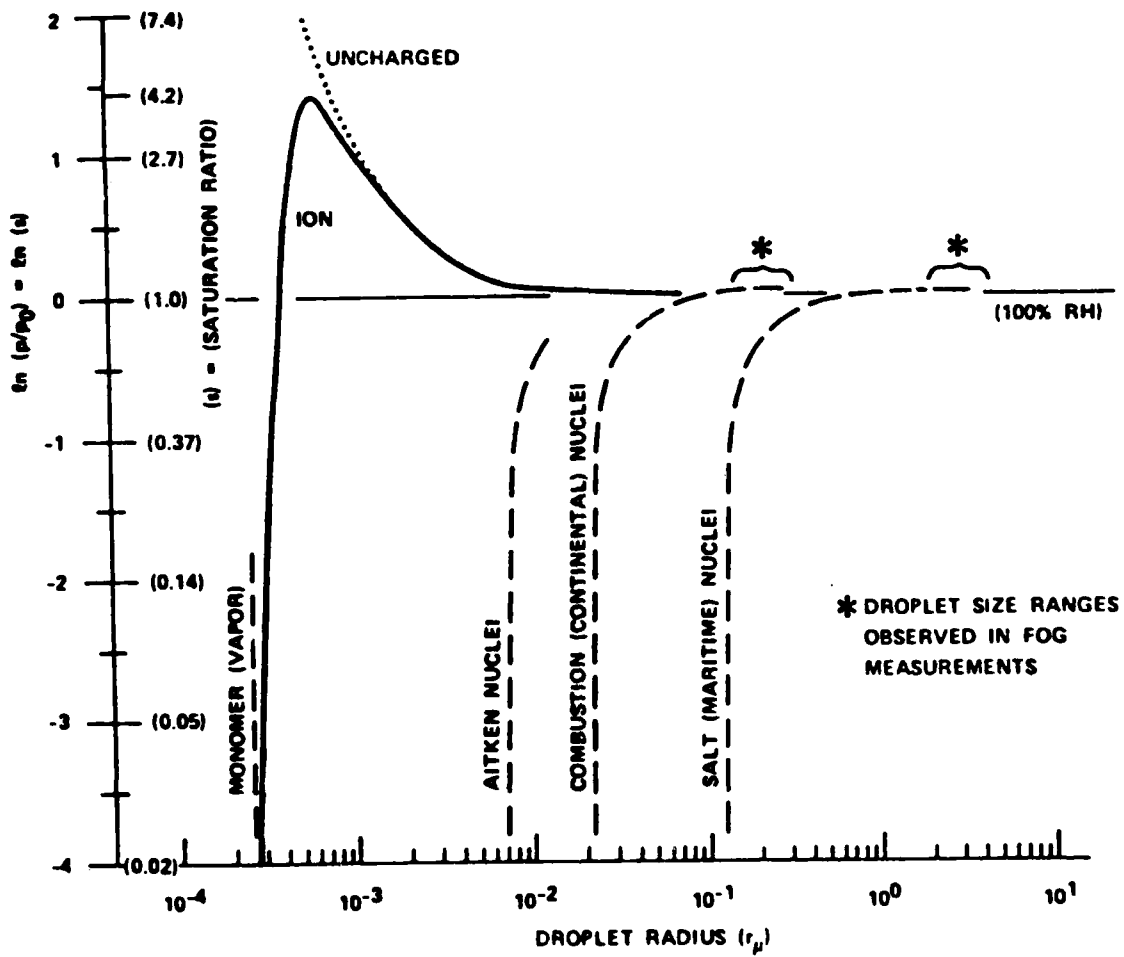


Figure 6. Vapor-Pressure Equilibria for Clusters and Water Droplets.

This discussion and Figure 6 make clear the apparent paradox in Carlon's original "fine aerosol" explanation of the water vapor continuum absorption. On the one hand, Carlon originally thought that condensation nuclei were necessary to account for the fine aerosols which he believed existed in moist air to produce the anomalous infrared continuum absorption and emission for which he had reported much evidence. But, Carlon noted, these aerosols were often too small to produce "noticeable optical scattering" in the visible wavelengths. The solution to the apparent paradox should be that the continuum absorption is due to ion clusters or ion hydrates which are represented by the "ion" curve in Figure 6 at atmospheric humidities equal to or less than  $s = 1.0$ .

The solution to the continuum problem, however, is not this straightforward. For one thing, it will be shown in this report that the numbers of ions in moist air are proportional to, but much smaller than, the populations required to explain the magnitude of the continuum absorption. The implication is that the vast majority of the infrared-active water clusters are neutral species like the dimer (Figure 3). Other evidence will be discussed to show that the responsible species are neutral, but much larger than the dimer and distributed differently than the dimer. Finally, there is the important effect of hydrogen bonding between water molecules which may have first been brought together by an ionic charge. If "cross-linking" occurs between water molecules first clustered by ions, then Equation 4 is lacking a term to express this. In his book, Wilson<sup>27</sup> states that Equation 4 "is clearly incomplete when, as for water, strongly polar molecules form an oriented surface layer." By the same token, the surface tension  $T$  is not independent of droplet radius as was assumed in constructing the "ion" and "uncharged" curves of Figure 6, nor is the term  $dT/dr = 0$ . Surface tension ceases to have meaning when droplets become so small as to have only a few hundred water molecules or less. In the vicinity of the "critical" cluster size or radius, and certainly for still smaller clusters, the latticelike molecular structures of water must be considered in ways which are completely foreign to classical thermodynamics. Hale and Plummer,<sup>28</sup> and many other cloud physicists, are actively engaged in finding molecular models which can explain nucleation phenomena for water.

Carlon is the only worker to find evidence of clusters in infrared spectra of water vapor, or in the phase-transitional realm of the vapor/liquid species, for example, in steam. Potter and Hoffman<sup>29</sup> measured anomalous infrared radiation from the vapor interface of boiling water in the 1.5-2.1  $\mu\text{m}$  wavelength region. This radiation considerably exceeded that from a blackbody at the same temperature. They termed this phenomenon "phase transition luminescence", and postulated that it was attributable to water clusters of at least 11 and 17 molecules. When these workers later repeated their measurements, using a non-"null" optical technique, their

results were much less definitive. This suggested to the present author that a nulled system was essential to observe these effects in his own radiometric measurements, which will be discussed in a later section of this report.

In the most recent literature, Wolynes and Roberts<sup>30</sup> made a brief attempt to relate the continuum absorption to molecular clustering using liquid water data, but Carlon<sup>31</sup> showed that their report simply repeated his own earlier findings. Carlon also took this opportunity to summarize a great deal of new work on cluster formation mechanisms, vibrational frequencies, and electrical properties of water vapor, showing their relevance to his own hypotheses. Carlon<sup>32</sup> also published a report discussing the differences in vapor and liquid absorption coefficients of water. He showed how this could be interpreted as *prima facie* evidence that clustering exists in both phases and can produce spectral activity not only in the infrared but at longer wavelengths as well.

### 3. METHODOLOGY

The problem investigated in this work has been summarized in the introduction, and the relevant literature has been reviewed. The hypotheses to be tested by experiment were the following:

- Water vapor contains complexes or "clusters" of water molecules which are phase-transitional species between the vapor and liquid phases. These complexes or clusters cannot be observed directly by any known experimental techniques.
- The modes of intermolecular or ion-molecular bonds in these clusters give rise to the anomalous infrared "continuum" absorption<sup>33</sup> and probably to similar phenomena at longer wavelengths as well. Calculating infrared spectral lines or bands of these modes should be possible.
- The clusters form and exist in water vapor by mechanisms which are describable using classical thermodynamic and chemical bond theory, even though certain aspects of classical thermodynamics (for example, surface tension) might not be applicable on the molecular scale.
- Many atmospheric water species are involved simultaneously in mechanisms which were not previously recognized as being closely interrelated, for example, infrared absorption/emission, cloud droplet nucleation, and electrical and electrostatic phenomena. Thus, there should be correlations between, for example, infrared absorption/emission and the electrical conductivity of water vapor or of moist air.

- Because of changes in distributions of water vapor and ions with altitude in the earth's atmosphere, these cluster effects might influence global weather and climate in complex ways not previously understood.

Experiments to test these hypotheses cannot establish unequivocally that they are correct or incorrect. But, a great deal of "circumstantial evidence" can be accumulated so that various hypotheses may be accepted as being correct with a high degree of confidence. Indeed, modern theories of atomic structure and many other fundamental "facts" concerning things, which cannot be measured directly, are based upon best hypotheses, which seem to be supported by experiment. This approach much be accepted in addressing the infrared continuum absorption and its explanation.

Thus, measurements of the anomalous infrared continuum absorption, even as functions of water vapor pressure and temperature, cannot establish unequivocally that this absorption is due to intermolecular modes of water clusters and not, for example, to Elsasser's pressure-broadened "wings" of vapor (monomer) absorption lines. Another kind of experimental evidence for the existence of clusters in water vapor is needed. For ion clusters, at least, this evidence could be found in the ion content of water vapor, as measured by electrical conductivity using sensitive cells, if the data could be correlated with infrared absorption as functions of water vapor pressure and temperature. Both infrared absorption and electrical activity of water vapor are enhanced in steam. Parallel investigations of steam using an infrared radiometer and electrical conductivity cells seem to be indicated, combined with a careful examination of all data in light of thermodynamic and chemical bond theory.

Any theory purporting to explain water cluster behavior in the liquid and vapor phases must operate not only near ambient temperatures, where mean cluster sizes should be relatively large and the density difference between phases were very great, but at temperatures including the critical temperature (374 °C), where the vapor and liquid phases become one, mean cluster size becomes unity, and the latent heat of vaporization becomes zero indicating that most or all intermolecular hydrogen bonds have been broken.

Because of all these considerations, the author decided to undertake parallel investigations of 4 different aspects of the cluster problem. Two of these investigations were experimental: (1) measurements of the infrared absorption and emission, and (2) electrical conductivity (ion content) of moist air at atmosphere pressure. These were carried out under conditions ranging from normal ambient to those of steam at 100 °C. Two of the investigations were theoretical. Simple oscillator models were considered for several water cluster configurations and a

complete study of the thermodynamics of clustering was performed up to the critical temperature of water.

### 3.1 Infrared Measurements.

The equipment used in these measurements has been described in the earlier literature.<sup>24,26,34</sup> The insulated, cylindrical, steel, test chamber is shown schematically in Figure 7. The chamber was 3.05 m in diameter and 3 m high. In some trials the 15 cm diameter viewports were windowless, and in other trials infrared-transmitting polyethylene film windows were used. Since precautions were taken to prevent steam condensation on the windows when used, identical results were obtained in either case.

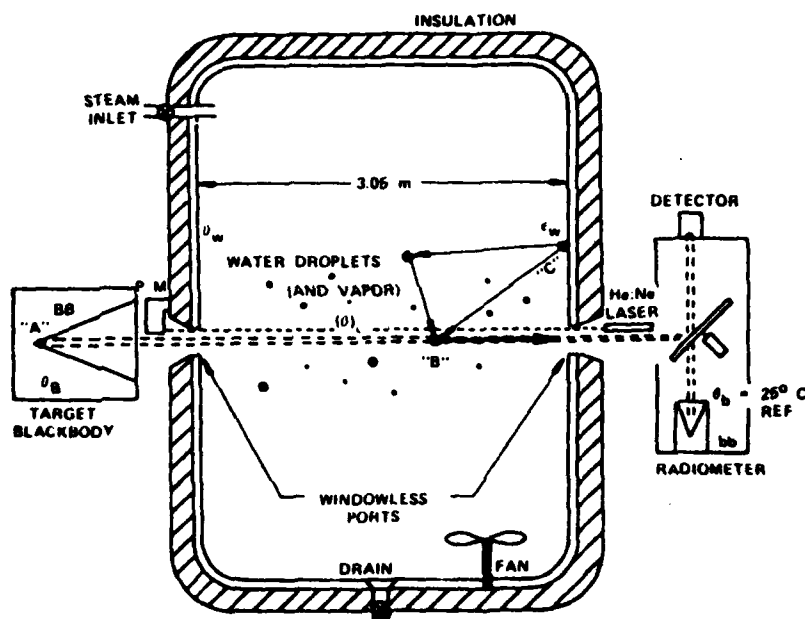


Figure 7. Steam Test Chamber, Vertical Section.

The viewports are considered windowless in the discussion here. The infrared radiometer was placed at one viewpoint. It had an internal reference blackbody (bb in Figure 7) which was maintained at ambient temperature  $\theta_b$ , near 25 °C through all calibration and steam trials described here. The radiometer had a field-of-view (FOV) 0.6° (10 mrad) square and a wavelength-scanning capability. The data reported here were taken in the 7-13  $\mu\text{m}$  wavelength region from scanned spectra (368 observations) and in trials where a fixed wavelength setting of 10  $\mu\text{m}$  was used (74 observations). The target blackbody (BB in Figure 7) was a thermostatted, waterjacketed, horizontal, blackened

steel cone with an emissivity,  $\epsilon_B$ , near 0.98 and an aperture 30 cm in diameter. A mirrored chopper in the radiometer allowed the detector alternately to view the radiometer reference blackbody (bb) at 25 °C, and the target blackbody (BB) at its temperature,  $\theta_B$ . A positive or negative demodulated radiometer signal could be obtained depending upon the sign of  $(\theta_B - \theta_b)$ . Since each trial was begun near ambient temperature ( $\theta_B = \theta_b = 25$  °C) and involved only higher temperatures, only positive-going radiometer signals were obtained. In blackbody calibration runs, the chamber was empty and  $\theta_B$  was elevated to various desired temperatures. In steam trials,  $\theta_B$  remained at 25 °C or was kept equal to  $\theta_b$  while the cloud temperature  $\theta_c$  was manipulated. Thus it was possible to express radiometer signals obtained either from the target blackbody (BB) or from the steam cloud in equivalent units of spectral radiant emittance ( $W_\lambda$ ), watts/cm<sup>2</sup>- $\mu$ m, for equivalent outputs. That is, a given steam cloud emission signal (emittance) for cloud temperature  $\theta_c$  could be compared directly to the emittance obtained in calibration of blackbody BB at the same temperature. By doing ratios of the emittances of the cloud and blackbody at that temperature, an "effective emissivity",  $\epsilon_\lambda = (W_\lambda)/(W_\lambda^\circ)$ , (unitless, where  $W_\lambda^\circ$  is the spectral radiant emittance of the blackbody) of the cloud could be determined and related to the concentrations of droplets and water vapor present in the chamber at that temperature.

A He:Ne laser (wavelength  $\lambda = 0.63$   $\mu$ m) and a power meter detector were aligned along an optical axis parallel to that of the radiometer and the target blackbody. The laser and radiometer thus could be used when steam was in the chamber to determine mean droplet size and mass (volume) concentration after the method of Carlon et al.<sup>35</sup> In addition, gravimetric samplers were used which gave droplet size distributions using sampling probes located along the optical axes. Thermocouples and calibrated glass thermometers were used to determine cloud temperature profiles ( $\theta_c$  values) within the chamber along the optical axes, and at the target blackbody BB to determine  $\theta_B$ . Thermocouples also were used between the steel chamber walls and their exterior insulation to measure the wall temperature,  $\theta_w$ . The time rate of change of chamber temperatures was much slower than the response times of the temperature-measuring devices during those portions of the experimental trials when most sensitive readings were made. In the "null" condition (that is,  $\theta_B \approx \theta_b$ ), the radiometer sensitivity could be maximized to detect signal changes corresponding to temperature differentials ( $\theta_B = \theta_b$ ) of less than 0.2 °C.

Saturated steam could be introduced into the chamber from a valved pipe at its top (Figure 7), and the condensate could be drained from the bottom of the chamber after each trial. A chamber fan could be used to insure uniform mixing during steam introduction, although the clouds were permitted to cool without forced convection in the experimental trials.

Because of the narrow FOV of the radiometer, it can be seen (Figure 7, where the FOV is exaggerated) that since the radiometer could not view the chamber wall directly, the only sources of modulated signal reaching the detector from the radiometer chopper were the surface of the target blackbody (BB) cone, for example, point A in Figure 7 provided the  $\theta_B = \theta_b$ ; cloud droplets viewed directly, for example, point B at cloud temperature  $\theta_c$ , provided  $\theta_c = \theta_b$ ; the wall of the chamber by scattering off droplets, for example, point C with emissivity  $\epsilon_w$  at temperature  $\theta_w$  in Figure 7. In the latter case at, least one scattering event is required, i.e., droplet B.

Calibration trials were run first for the target BB, using an empty chamber, by elevating temperature  $\theta_B$  while keeping  $\theta_b \approx 25^\circ\text{C}$  and scanning wavelengths at each temperature. The spectral radiant emittance of the blackbody,  $(W^\circ_\lambda)$ , was recorded for each wavelength (0.5  $\mu\text{m}$  intervals) at each temperature. Thus, during actual steam trials, the effective emissivity of a cloud at temperature  $\theta_c$  could be taken as the ratio  $\epsilon_\lambda = (W_\lambda)\theta_c / (W^\circ_\lambda)\theta_B$ , where  $\theta_B = \theta_c$ ; that is, the effective emissivity of the cloud was the ratio of its observed spectral radiant emittance at some temperature, to that of the blackbody ( $\epsilon_B \approx 1.0$ ) as measured at the same temperature and wavelength.

The time and temperature history of a typical steam trial is shown in Figure 8. While steam was introduced into the chamber for 10 min, the wall temperature  $\theta_w$  rose from ambient ( $25^\circ\text{C}$ ) to  $40^\circ\text{C}$ . The target BB was kept at the same radiometric temperature as the radiometer reference blackbody (bb) so that no signal was detected from the target, and a flat spectral base line was obtained; that is, a radiometric null existed with  $\theta_B \approx \theta_b$ . When the steam flow was shut off, the temperature of the steam cloud in the chamber ( $\theta_c$ ) fell to  $40^\circ\text{C}$  within the next several minutes. During the very interesting cool-down periods for the next 20-30 min of each trial, the comparatively stable wall temperature  $\theta_w$  dropped to about  $35^\circ\text{C}$ , while the cloud temperature  $\theta_c$  fell more rapidly with the last residual steam droplets seen at about  $30^\circ\text{C}$ , illuminated by the He:Ne laser beam. At about  $37^\circ\text{C}$  in each trial, the wall and cloud temperatures were equal.

Optical and gravimetric steam droplet concentration determinations were made repeatedly during the cool-down periods. Saturation humidity was maintained in the chamber nearly until the end of each trial when the residual droplets evaporated. In Figure 8, the  $C_D$  values refer to the droplet mass (volume) concentration ( $\text{g}/\text{m}^3$ ) for the specified times and cloud temperatures. At each cloud temperature, a typical  $C_D$  value was quite reproducible from one steam trial to the next. This liquid water content is conveniently expressed in CL units ( $\text{g}/\text{m}^2$ ), where CL is the product of  $C_D$  and the optical path length of the chamber L in meters (3.05 m in other trials reported here).

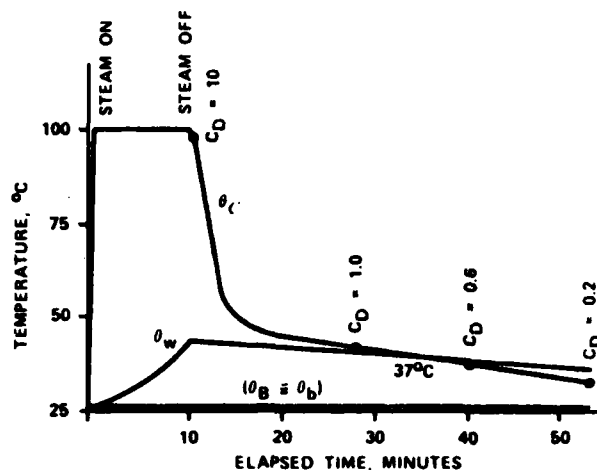


Figure 8. Time-Temperature History of Typical Steam Trial;  
 $C_D$  = Droplet Mass (Volume) Concentration,  $g/m^3$ .

### 3.2 Electrical Conductivity Measurements.

The existence of small, hydrated ions in moist atmospheres is well known.<sup>36,37,38,39</sup> A typical hydrated ion consists of 10 or 12 water molecules<sup>40</sup> clustered about a single ionized molecule in the fashion shown in Figure 2, and kept together by the charge.<sup>41</sup> Such ions have mobilities ( $\mu$ ) on the order of 1-2  $cm^2/volt\text{-}sec$ .

Typical cells for the measurement of the electrical conductivity of air, such as the Gerdien tube,<sup>42</sup> have modest dimensions and poor sensitivities. A new kind of cell was designed and fabricated for the measurement discussed here. This cell had 40 parallel steel plates with a total area ( $A$ ) of  $6.6 \times 10^4 \text{ cm}^2$  spaced  $L = 0.66 \text{ cm}$  apart. A compensating cell also was fabricated with an identical insulator configuration but with a much smaller plate area ( $2600 \text{ cm}^2$ ), so that conductivity measurements of moist air could be corrected for electrical leakage of the insulators. Together the cells allowed very sensitive measurements to be made of the electrical conductivity and, hence, of the ion content of moist air between the cell plates, over a wide range of temperatures and humidities. Insulator leakage also was studied. By designing both cells optimally, and then by dealing directly with residual leakage rather than by going to extraordinary lengths to avoid it, good experimental reproducibility was obtained.

It was desirable to study the ion content of moist air because it was observed in an unpublished report by Carlon, Do Clusters Contribute to the Infrared Absorption Spectrum of Water Vapor, that the functional dependence of the infrared continuum absorption coefficient,  $(C_s^0)_\lambda$  ( $\text{cm}^2/\text{molecule-atom}$  of water vapor), upon temperature is given almost precisely by:

$$(C_s^0)_\lambda = \frac{K_s \sqrt{K_w}}{P_w} \quad (5)$$

where  $K_s$  is a constant,  $p_w$  is the partial pressure of water vapor, and  $K_w$  is the ion product of water at the observation temperature. This function dependence may be entirely fortuitous, but it also allows the possibility that thermal energy in water itself, as reflected in the ion product, may be one mechanism of ion and cluster production in water vapor. Holzapfel<sup>43</sup> has found that the ion product of water is density-independent and can be calculated as a function of temperature for the simple empirical relationship:

$$K_w = \exp \left( -8.17 - \frac{7156}{\theta_k} \right) \quad (6)$$

It is possible to measure the ion content of moist air and relate it to the ion content expected from the dissociation of water itself. Finally, the dependencies of ion populations upon temperature and humidity could be compared to the dependence of the infrared continuum absorption upon these same variables, to determine whether correlations could be found linking ion or ion-induced water cluster species to the continuum absorption.

The current density ( $j$ ), amp/cm<sup>2</sup>, for singly-charged ions is:

$$j = N n u E, \quad (7)$$

where  $N$  is the number of ions per cm<sup>3</sup> or air,  $E$  is the field strength (volts/cm), and  $n$  is the value of the electronic charge ( $1.6 \times 10^{-19}$  coulomb). Hence, for the cells described here, the direct current (DC) resistance or reciprocal conductance in megohms ( $R_{\text{meg}}$ ) is related to  $N$  by the expression:

$$N = \frac{L}{A} \cdot \frac{10^{-6}}{R_{\text{meg}} n \mu} \quad (8)$$

or, approximately:

$$N \approx \frac{3 \times 10^7}{R_{\text{meg}}} \quad (9)$$

for the large conductivity cell where  $L/A = 0.66/6.6 \times 10^4 = 10^{-5} \text{ cm}^{-1}$ . The large and small compensating cells are shown in Plate 1. The large cell consists of 40 1-mm thick steel plates, each 41 cm square. Alternating plates are connected to either of 2 bus wires running the length of the cell, somewhat in the fashion of the plates in an automotive storage battery but with moist air as the electrolyte. The plates were supported by five 8-mm diameter resin impregnated fiberglass rods with nylon spacers 0.66-cm thick. These materials were selected for their high electrical resistance but were not the only materials tried. Teflon rods and spacers were used in other cells which were constructed during the 2-year period over which these tests were performed. However, the teflon insulators gave extremely troublesome surface effects. They were abandoned in favor of the materials described above, which gave reproducible results and negligible shunting resistances compared to those of typical moist air samples. Nevertheless, care was taken to minimize contact area between rods, spacers, and steel plates. As a result, despite the very large dimensions of the cell, leakage resistance at ambient temperature and 50% relative humidity ( $s = 0.5$ ) averaged  $10^{10}$ - $10^{11}$  ohms.

Exactly the same insulator configuration was used in the small, compensating cell (Plate 1) as in the large cell. Only the area of the overlapping plates was different. The "cell factor",  $L/A$ , of both cells was checked after cell fabrication by treating the cells as capacitors with air dielectrics and determining their electrical capacitances with an impedance bridge, from which:

$$\frac{L}{A} = \frac{8.85 \times 10^{-8}}{C_{\mu\text{f}}} \quad (10)$$

where  $C_{\mu\text{f}}$  is the capacitance in microfarads. Tests conducted over wide ranges of temperature and humidity confirmed that the electrical leakage characteristics of the insulators in both cells were nearly identical. In all experiments, both cells were always mounted and measured in the same way. Thus, differences between the large and small cell resistances in actual experiments could be attributed solely to the conductivity of the moist air between the cell plates. In all experiments where water vapor condensation on the insulators was possible, the compensating cell was always placed in the most disadvantageous position within the test chamber. That is, the

position where condensation, if it occurred at all, would affect the compensating cell insulators to a greater extent than the large cell insulators. In this manner, conductivities attributed to moist air were always conservative if, in fact, any condensation occurred.

Extensive testing was done with the compensating cell to study insulator leakage effects as functions of temperature and humidity. The most interesting observation was that insulator resistance plots had the same general shapes as moist air plots, except that the magnitude of moist air conductances were about 10-30 times greater than those of the insulators. In other words, the data indicated that the same kinds of ionic species were present on the insulators as in the air, and were largely responsible for the insulator leakage. But under high temperature and near-saturation humidity conditions, the ion populations on the insulators never approached those between the plates of the large cell (in the air).

Field strengths ( $E$ ) of 1 v/cm - 100 v/cm were used in the work reported here, after it was verified that Ohm's Law was obeyed, that no additional ions were produced by the field. A cell bias voltage of 20 v was selected for general use. Because of the large dimensions of the cells, it was found that electrometers or other extremely high-impedance devices were not required for sensitive measurements. In most cases, cell resistances could be determined easily by using a vacuum-tube voltmeter with an 11 megohm input impedance directly in series with the bias supply and the cell under test, and measuring the voltage division. The polarity of the bias voltage had little effect upon cell resistance. A small voltage was sometimes measured on the large cell (about 0.02 v) in the absence of bias. But, this was negligible compared to voltage measured during normal operation. The 0.66 cm cell plate spacing was chosen to allow adequate circulation of moist air between the plates and to reduce the likelihood of short-circuiting. When the cells were placed in constant use, it was found that short circuits sometimes would occur due to "whiskers" of contamination which bridged a spacer between two plates. But, without exception, it was found that the cell could be "cleaned" and restored to normal operation by the momentary application of a 400 v bias directly across the plates. Therefore, this procedure was routinely adopted for use before experiments where unusual sensitivity was required.

The steam test chamber or cabinet is shown in Plate 2. Only the large cell is shown in the cabinet in this photograph. The small (compensating) cell was always placed closer to the point of steam introduction than was the large cell, during all experiments, for reasons which have already been explained. All data reported in this report were taken under steady-state conditions with DC fields and stagnant, moist air between the cell plates. These conditions were quite different from those normally used with the Gerdien tube, where the conductivity of a

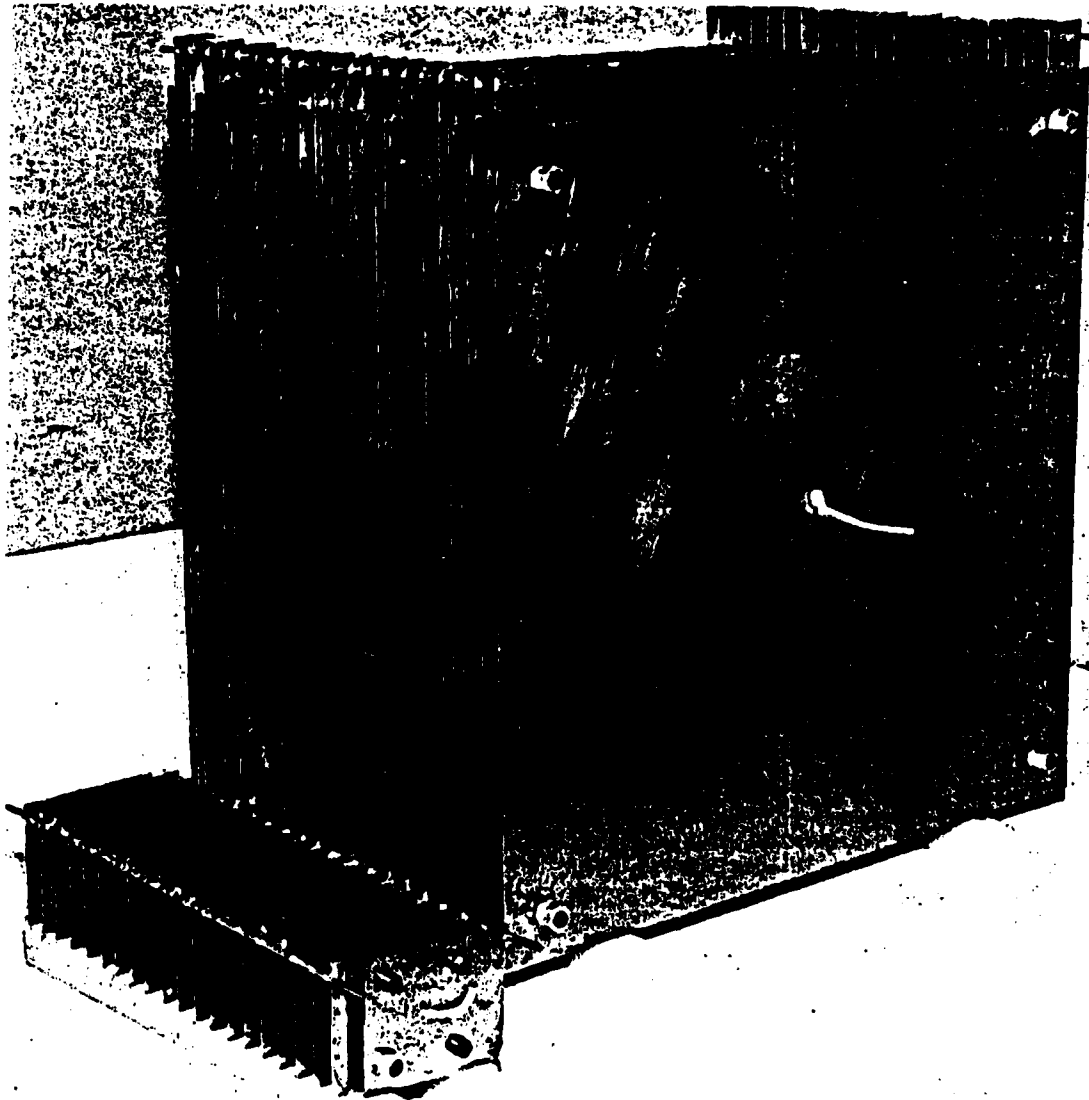


Plate 1. Conductivity Cells: Both Cells Have Identical Insulator Configurations. For Scale, the Large Cell Plates Are 41 cm on Each Edge.

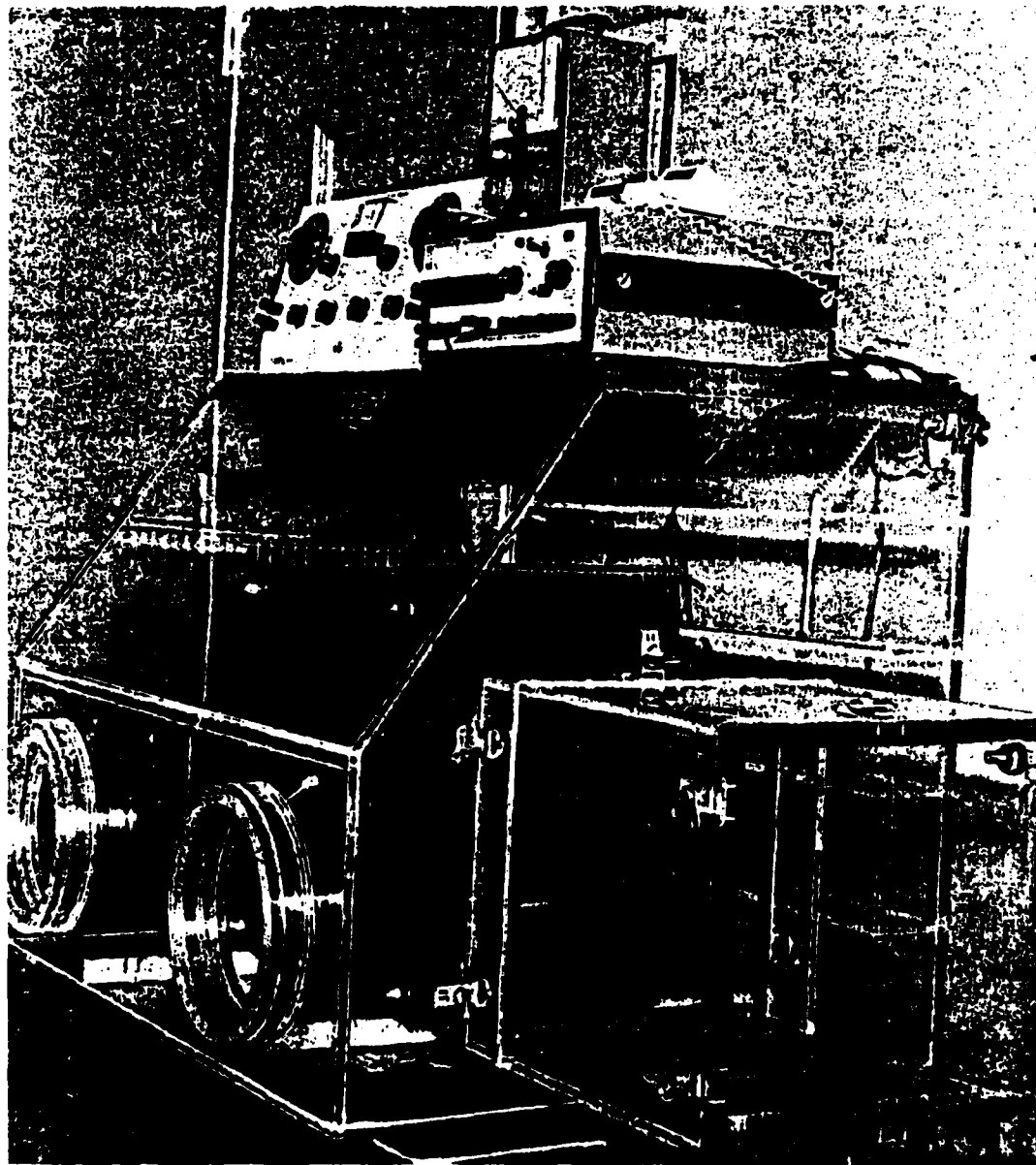


Plate 2. Large Conductivity Cell in Test Cabinet, with Instrumentation.

flowing gas stream is sampled with as little disturbance to the sampled volume as possible.

Water was boiled at 100 °C in a side compartment of the test cabinet. The vapor was admitted through a slit into the large compartment containing the cells, passing first over the small, compensating cell and then over the large, sensitive cell. Resistances of both cells were constantly monitored. When sufficient water vapor had been admitted, the slit was closed and the cell compartment was sealed at atmospheric pressure. Provisions were made to heat the air in the sample compartment with a small hotplate, and to vent the compartment to room air when necessary. Each moist air sample was allowed to equilibrate before readings were taken for retention. The amount of water vapor entering the sample compartment was insufficient to cause appreciable heating. About a 1 ° increase was typical between the initiation and completion of steam introduction, for example, from 26 °C - 27 °C.

### 3.3 Simple Cluster Models.

The infrared-active modes associated with many kinds of water clusters would be extremely complex, requiring sophisticated computational techniques to describe them, such as a normal coordinate analysis.<sup>19,44</sup> But, it is found that relatively few modes are associated with the infrared continuum absorption. Consider a simple harmonic oscillator like the one shown schematically in Figure 9, consisting of two masses,  $M_1$  and  $M_2$ , connected by a resilient bond. Carlon<sup>45,46,47</sup>, in an unpublished report, "Do Clusters Contribute to the Infrared Absorption Spectrum of Water Vapor", has shown that the simplest cluster modes can be described for this model by the equation for simple harmonic oscillators:

$$\lambda_c = 2 \pi C_v \sqrt{\frac{1}{K} \left( \frac{M_1 M_2}{M_1 + M_2} \right)} \quad (11)$$

where  $C_v$  is the velocity of light,  $K$  is a constant (force constant) and  $\lambda_c$  is the resonant wavelength,  $\mu\text{m}$ .

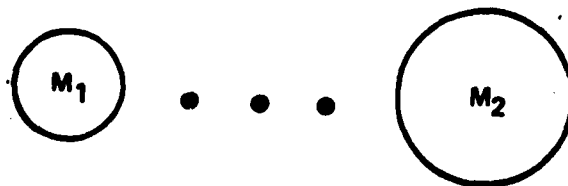


Figure 9. Simple Oscillator Model.

The simplest kind of polymolecular water complex or cluster, for illustrative purposes using this model, is the ion cluster, where any number of water molecules can swarm about a positive or negative ion to share the charge. Examples for cluster sizes of 6 water molecules ("c" = 6, where c is defined as the cluster "size") are shown schematically in Figure 2. This swarming and clustering, according to Israel,<sup>50</sup> occurs in less than a microsecond when an ion is exposed to water vapor. All bonds in a given ion cluster having a single molecular layer or "shell" about the ion, as in Figure 2, will have approximately the same resonant wavelength,  $\lambda_c$ , since each water molecule will act like one mass in Equation 11 or in Figure 9 (where the dots represent an ion-molecule bond or shared charge), while the remaining water molecules and the ion together will form the other, larger mass. Thus  $M_1$  and  $M_2$  can be written:

$$M_1 = M = 18, \text{ and} \quad (12)$$

$$M_2 = m + (c-1)M \quad (13)$$

if  $M$  is the molecular weight of water ( $M = 18$ ) and  $m$  is the molecular weight of the ion which "induced" formation of the cluster. Since the ionic charge,  $F$ , which holds the cluster together is divided or averaged among "c" water molecules so that the constant in Equation 11 is  $K = F/c$ , this equation can be rewritten as:

$$\lambda_c = 2\pi C_v \sqrt{\frac{c \cdot M [m + (c-1) M]}{F [m + c \cdot M]}} \quad (14)$$

If a new constant is defined such that  $K' = 2\pi C_v \sqrt{M/F}$ , then Equation 14 is found to take several forms depending upon the mass of the ion,  $m$ , compared to the mass of each water molecule:

$$\lambda_c = K' \sqrt{(c-1)} \quad (\text{when } m \approx 0) \quad (15)$$

$$\lambda_c = K' \sqrt{\frac{c^2}{c+1}} \quad (\text{when } m \approx M) \quad (16)$$

$$\lambda_c = K' \sqrt{c} \quad (\text{when } m \gg M) \quad (17)$$

It is also observed that, regardless of the mass of the ion,  $m$ , as the cluster size,  $c$  becomes larger, Equations 15-17 can be represented by a very simple equation:

$$\lambda_c = K'' \sqrt{c} \quad (\text{when } c \gg 1) \quad (18)$$

where  $K''$  is another constant which can be empirically determined.

Water molecules swarmed about an ion (as in Figure 2) also would experience intermolecular attractions due to hydrogen bonding. These attractions would result in "cross-linking" of water molecules as the cluster size,  $c$ , increased. Hydrogen bonding energized between water molecules are such (typically 0.2 ev)<sup>8</sup> that by the time a water cluster has attained a size of  $c = 4$  or 5 water molecules, the hydrogen bonds have become more important than the ionic charge (typically 1.0 ev)<sup>49</sup> in holding the cluster together. Thus, even if the ionic charge is neutralized by collision (or possibly by combination with an oppositely-charged cluster forming a new cluster with the combined mass of both), stable hydrogen-bonded neutral water clusters can survive and even continue to grow in the vapor phase. Experimental evidence<sup>50,51</sup> indicates that these neutral water clusters can have lifetimes of minutes to hours. As new bonds are formed with the clusters, new modes, and new resonance lines are added to their infrared spectra. While ions are necessary for the formation of the clusters discussed here, they are not necessary for the infrared absorption of the clusters thus formed. The infrared spectrum due to clusters can be considered as the composite of all lines contributed by all modes (ion-molecule and intermolecular) of clusters of all different sizes and geometries present in the distribution of all such species present in water vapor at a given temperature and partial pressure. Understandably, this absorption is continuumlike.

#### 3.4 The Thermodynamics of Clustering.

The similarities between the spectra of water vapor (Figure 4) and liquid water (Figure 5) have been discussed earlier in this report, as have the reasons why the continuum absorption would seem to be explicable due to traces of "fine aerosol" in the vapor phase. But, there are other spectral differences between water's phases which should now be discussed. Hale and Querry<sup>52</sup> have made careful measurements of liquid water absorption, and their data are redrawn in Figure 10.

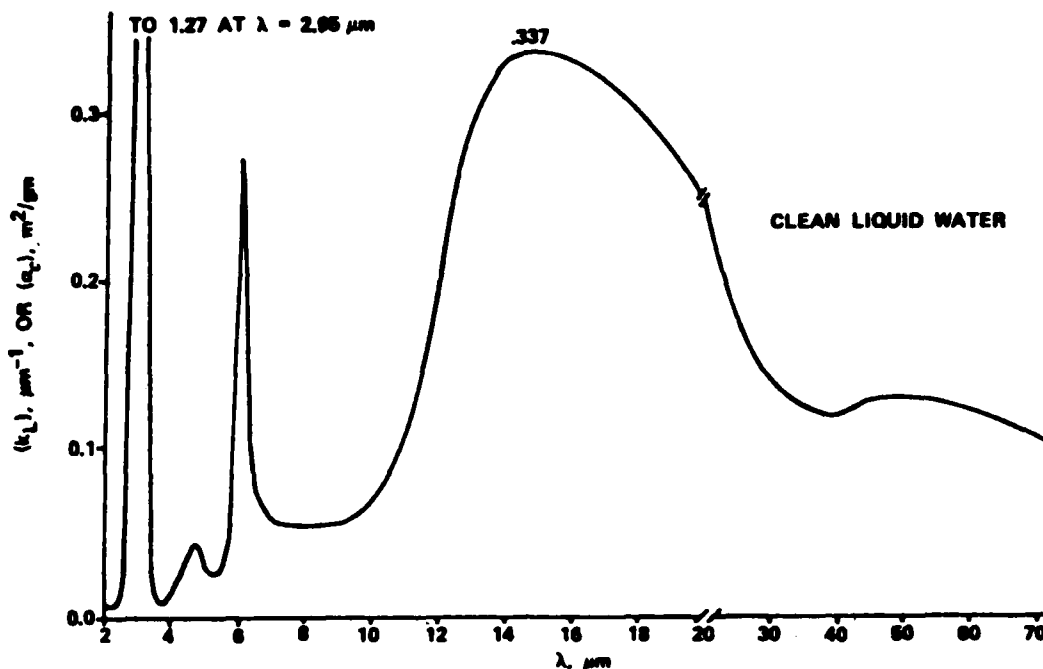


Figure 10. Absorption Coefficient Spectrum for Liquid Water.

This figure shows, much more clearly than Figure 5, two bands in liquid water which do not appear in spectra of water vapor. The small band near  $4.7 \mu\text{m}$  is attributable to hydronium ion,  $\text{H}_3\text{O}^+$ ,<sup>53,54,55</sup> while the enormous peak near  $15 \mu\text{m}$  is attributable to the "librational" modes of hydrogen bonds in the latticelike (clustered) structure of liquid water.<sup>56</sup> Luck<sup>57</sup> has shown that liquid water is about 85% hydrogen-bonded at  $20^\circ\text{C}$ . Thus, the peak intensity of the absorption at  $15 \mu\text{m}$  should be directly proportional to the numbers of hydrogen bonds per gram of liquid water. At the peak, this absorption has a coefficient  $k_L = 0.337 \mu\text{m}^{-1}$  or  $\text{m}^2/\text{g}$ . This probably also can be taken as a maximum value for hydrogen bonds in water clusters, if it is assumed that hydrogen bonds have a similar nature in water clusters and in liquid water. In the vapor phase, of course, a correction must be made for the tiny fraction of water molecules which is actually clustered, compared to the nearly complete clustering of the liquid phase. This fraction, designated by  $(n_c)_v$ , has been stated to be on the order of  $10^{-5}$  or more, compared to the fraction hydrogen-bonded or clustered in the liquid, designated  $(n_c)_L$ , which has been stated to be about 0.85 at  $20^\circ\text{C}$ .

The infrared continuum absorption coefficient,  $(C_s^0)_\lambda$ , as compiled by Roberts et al.<sup>33</sup> from the data of many workers, is shown in Figures 11 and 12 for measurements at 8-13 m in the

infrared atmospheric "window" there and for the region extending to longer wavelengths and toward the water "rotational band" beyond 30  $\mu\text{m}$ . The spread of data points (circles) in Figure 11 is significant and meaningful, and it will be discussed in a later section.

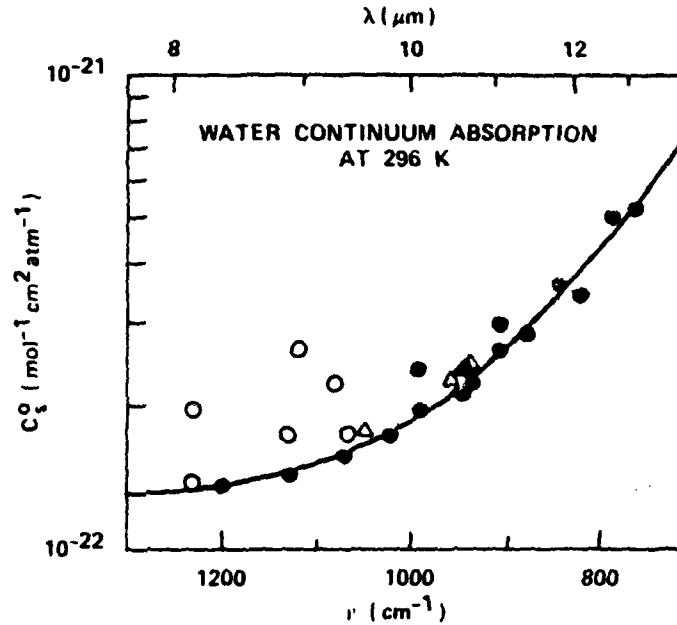


Figure 11. Infrared Continuum Absorption Coefficient, 8-13  $\mu\text{m}$ .

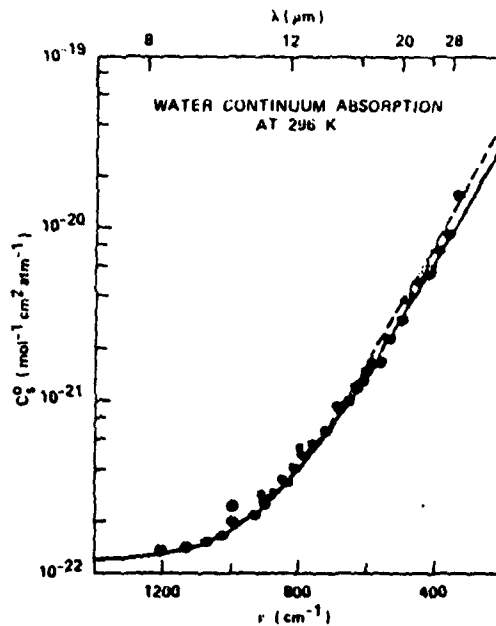


Figure 12. Infrared Continuum Absorption Coefficient, 8-28  $\mu\text{m}$ .

From these data and the liquid water data of Figure 10 (specifically the peak absorption coefficient due to clustering at 15  $\mu\text{m}$ ), it is possible to estimate the minimum fraction of water molecules which must be clustered in the vapor phase to account for the continuum absorption. The number of molecules per gram of liquid water is  $6.02 \times 10^{23}/18 = 0.334 \times 10^{23}$ . If  $(n_c)_L$  is the fraction of these molecules actually clustered or hydrogen-bonded in the liquid, then the number of bonded molecules per gram of the liquid is  $0.334 \times 10^{23}/(n_c)_L$ . The molecules will have a maximum absorption coefficient in this wavelength region of  $0.337 \text{ m}^2/\text{g}$ , and thus the maximum absorption coefficient per molecule of water will be  $0.337/0.334 \times 10^{23} (n_c)_L$  or approximately  $10^{-23}/(n_c)_L \text{ m}^2$  per bonded molecule, which is the same as  $10^{-19}/(n_c)_L \text{ cm}^2$  per bonded molecule. If the bonded water molecules are now dispersed in water vapor as clusters, where they represent a fraction  $(n_c)_v$  of all water molecules present, their absorption coefficient will be approximately  $10^{-19}(n_c)_v/(n_c)_L \text{ cm}^2$  per molecule of water vapor. By including a correction for total water vapor concentration, this result can be used to write:

$$(C_s^0)_\lambda = \frac{7.6 \times 10^{-17} (n_c)_v}{(s) (P_0)_\theta (n_c)_L} \quad (19)$$

where  $p_0$  is the saturation vapor pressure at temperature  $\theta$ . If values of  $(C_s^0)_\lambda$  in the 10  $\mu\text{m}$  wavelength region are substituted in Equation 19, it is found that the dependence of the minimum value of  $(n_c)_v$  upon the saturation ratio "s" at some temperature is:

$$(n_c)_v = K_\theta \cdot s \quad (20)$$

where  $K_\theta$  is equal to  $6 \times 10^{-5}$  at 20  $^\circ\text{C}$ ,  $46 \times 10^{-5}$  at 85  $^\circ\text{C}$ , and  $92 \times 10^{-5}$  at 115  $^\circ\text{C}$ . The mass fraction of water vapor which is clustered increases with temperature. The value  $(n_c)_v = 6 \times 10^{-5} (s)$  at 20  $^\circ\text{C}$  for example, is smaller than the cluster fraction  $10^{-3}$  to  $10^{-4}$  estimated by Carlon from his "fine aerosol" assumptions, but it does not differ greatly. This minimum calculated value is based upon the value of  $(C_s^0)_\lambda$  at one wavelength. Since the continuum absorption extends over a broad range of wavelengths, it is understandable that the total cluster population, accounting for all absorption at all wavelengths, should be larger than the fraction necessary to explain absorption only at a selected wavelength. If the mass fraction of vapor which is clustered is known from Equation 20, then the actual cluster concentration in the vapor is the product of the mass fraction and the vapor concentration, or:

$$C_c = (n_c)_v C_1 = \frac{(n_c)_v k s p_o}{\theta_k} = \frac{k K (s)^2 p_o}{\theta_k} \quad (21)$$

where  $C_c$  is the cluster mass (volume) concentration,  $g/m^3$ ,  $C_1$  is the water vapor concentration,  $g/m^3$ ,  $k$  is a gas constant numerically equal to 289,  $K$  is  $K_0$  in Equation 20 and  $\theta_k$  is the Celsius temperature. Thus, at a given temperature, the cluster concentration should be proportional to  $(s)^2$ . In other words, the concentration of these species in water vapor could determine the  $(s)^2$  dependency of the infrared continuum absorption.

The author has found that the cluster fraction can also be expressed in a form of the Clausius-Clapeyron equation which gives very good agreement between observations and temperature dependency of this fraction required for thermodynamic consistency up to the critical temperature:

$$\ln(n_c)_v = C - \frac{\Delta H}{R\theta_k} \quad (22)$$

$C$  is an empirical constant,  $\Delta H$  is the latent heat of vaporization of water, and  $R$  is a gas constant = 1.987 g-cal/mole-°K. When  $C$  is evaluated and the equation is rewritten, it is found that the cluster fraction can be expressed as:

$$(n_c)_v = \exp \left( -1.04 - \frac{4.34 \Delta H}{\theta_k} + \ln(s) \right) \quad (23)$$

Equation 23 has a form not unlike that obtained empirically for the temperature correction of the continuum absorption by Roberts et al.<sup>33</sup> The combination of Equation 23 with Equation 19 yields a new expression:

$$(C_s)_\lambda = \frac{7.6 \times 10^{-17}}{p_o(n_c)_L} \exp \left( -1.04 - \frac{4.34 \Delta H}{\theta_k} \right) \quad (24)$$

If Equation 23 for  $s = 1.0$  is plotted with the temperature dependence of the cluster fraction in liquid water,  $(n_c)_L$ , after Luck,<sup>57</sup> it is found that the clustered fractions of both phases should converge at the critical temperature. This is shown in Figure 13. Perhaps it is also useful to present evidence that the latent heat of vaporization of water consists of two components. One component includes the interattractive forces common to all liquids, while a second (larger) component apparently is associated with the hydrogen bonding which is

peculiar to water. This is illustrated in Figure 14, where  $\Delta H$  is plotted as a function of the weight fraction of "O-H" in various molecules. Pure water has a fraction of 1.0 (corrected here for the fraction of hydrogen bonds,  $(n_c)_L$ ), while nonane represents the 0.0 fraction. In between, various straight chain alcohols are represented by different fractions. It can be seen that the latent heat,  $\Delta H$  (which is also temperature-dependent for the data represented) falls rapidly with falling hydrogen-oxygen content of the molecule, until it attains a level typical of many other substances which are not hydrogen-bonded, as the weight fraction of O-H approaches zero. This result is interesting for two reasons. First, it shows that interattractive or surface tension forces in water are closely linked to the latent heat of vaporization. This gives justification to the use of the latent heat in thermodynamic expressions which seek to relate bond energies in vapor-phase water clusters to those in liquid water. That is, it appears to help justify the assumption that hydrogen bonds are similar in both phases, and that liquid water data can be extrapolated to water clusters. Second, it may help to explain why Carlon<sup>32</sup> found much smaller phase transition changes in the absorption coefficients of straight-chain alcohols in the infrared than he had found for water. This suggested that clustering was far less extensive in alcohols than in water and, if hydrogen bonding is important in clustering, the reduction in hydrogen bonding with greater alcohol chain length, as reflected in the latent heat in Figure 14, might explain this result.

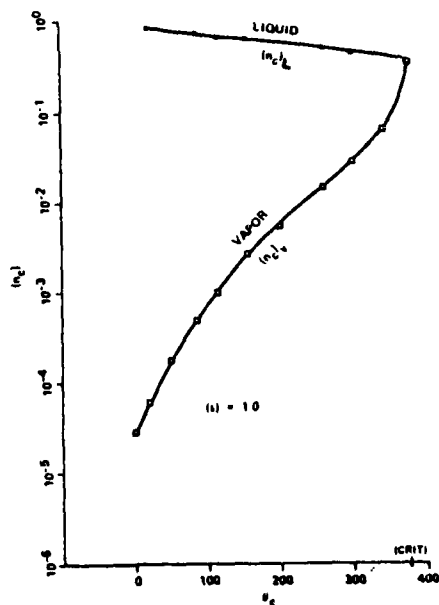


Figure 13. Fraction of Water Molecules Clustered In Liquid Water,  $(n_c)_L$ , Top Curve, and In Water Vapor,  $(n_c)_v$ , Lower Curve, vs. Temperature.

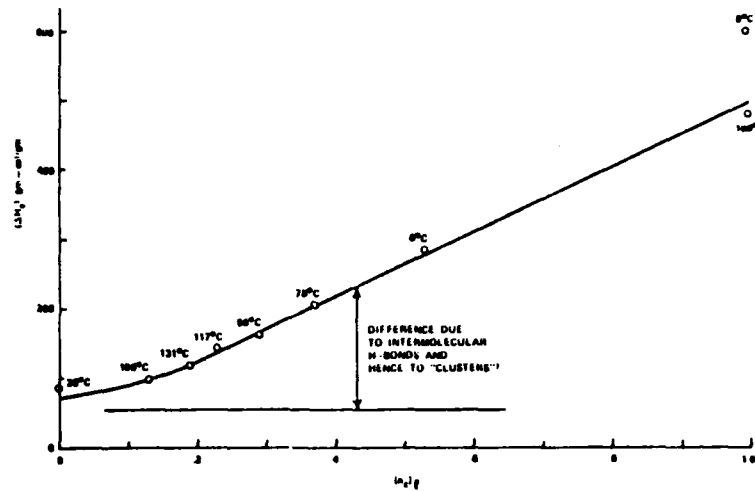


Figure 14. Latent Heat of Vaporization,  $\Delta H$ , vs. Weight Fraction of "O-H" in Molecule; Pure Liquid Water Corresponds to  $(n_c)_L = 1.0$ .

Measurements have been made of actual distributions of water ion clusters including  $Pb^+(H_2O)_c$ .<sup>49</sup> These data are shown in Figure 15 and can be used in the following discussion.

DISTRIBUTION OF LEAD ION-WATER CLUSTERS AT 300°K

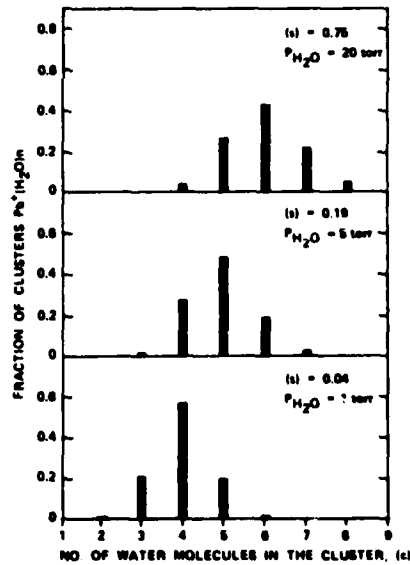


Figure 15. Distributions of  $Pb^+(H_2O)_c$  Clusters Measured by Castleman and Tang.<sup>49</sup>

Unlike those for homogeneous clusters, number distributions of ion clusters (and probably of neutral clusters which they produce) are peaked at some mean cluster size,  $c_\mu$ , where this mean varies with the saturation ratio (at some temperature) approximately as:

$$c_\mu = k \ln (s) + K \quad (25)$$

where the empirical constant  $K$  is the mean cluster size at  $s = 1.0$ , and  $k \ln (s)$  reaches a value of  $(1 - K)$  at some low value of "s" where "clustering" of more than one water molecule is no longer expected, that is, where  $c = 1$ . For example, the data of Figure 15 indicate that for lead ion at 300 K,  $k = 0.68$  and  $K = 6.2$  in Equation 25. Empirical evidence for the water clusters found in typical atmospheres suggests that these constants in that situation are approximately  $k = 1.0$  and  $K = 1.0$ .

The Calusius-Clapeyron equation is:

$$\ln(p_0) = - \frac{\Delta H}{R\theta} + C \quad (26)$$

where  $p_0$  is the saturation vapor pressure,  $C$  is a measured constant value to 21 for water,  $R = 1.987$  gm-cal/mole-degree, and  $\Delta H$  is the mean latent heat of vaporization for each temperature, gm-cal/mole. Equation 25 can be written:

$$c_\mu = k \ln (p) - k \ln (p_0) + K, \quad (27)$$

where  $(p)$  is the partial pressure of water, so that:

$$c_\mu = k \ln (p) - k \left( - \frac{\Delta H}{R\theta} + 21 \right) + K, \text{ or } \quad (28)$$

$$c_\mu = k \left[ \ln(p) + \frac{\Delta H}{R\theta} - 21 \right] + K. \quad (29)$$

Equation 29 is plotted in Figure 16 for  $k = 1.0$  and  $K = 10$ . If the interpretation is made that atmospheric water clusters are formed on ions and held together by hydrogen bonds which are at least similar to those found in liquid water, Equation 29 should give a first approximation of the dependency

of  $c_{\mu}$  upon temperature. This dependency is seen in Figure 16 to be a negative one, with all hydrogen bonds broken (and thus, all clusters which are held together only by hydrogen bonds dissociated) at the critical temperature, if this simple model is a reasonably valid one.

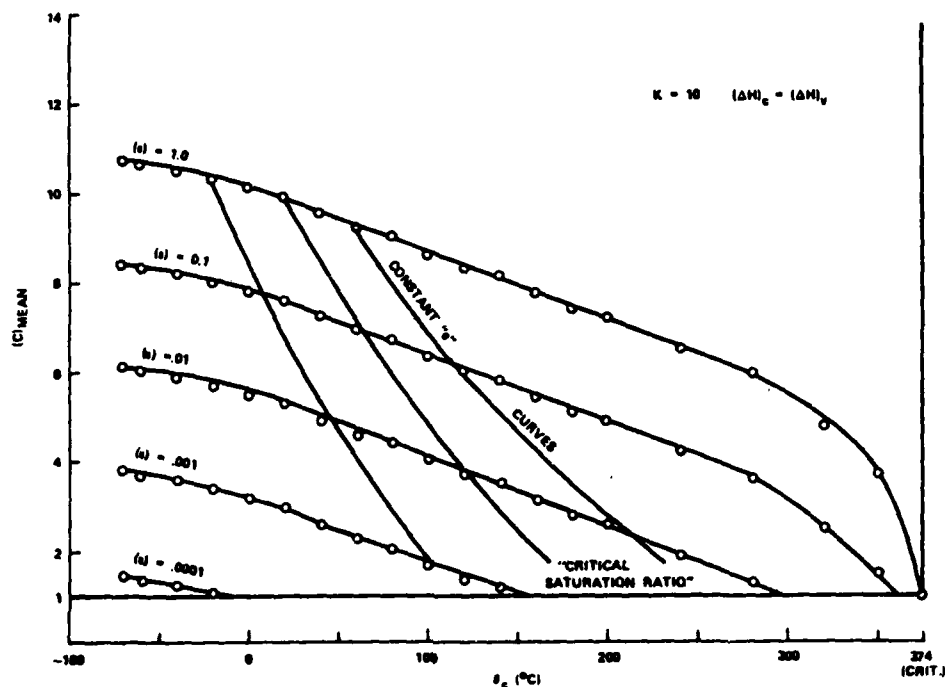


Figure 16. Calculated Curves from Equation 29 for  $k = 1.0$  and  $K = 10$ .

From the discussion to this point, it is possible to show in one figure the best available estimates of the populations of various water species in the vapor phase at various temperatures. This is done in Figure 17, for  $s = 1.0$ , where the "discrepancy" between the numbers of ions per  $\text{cm}^3$  and the number of water clusters per  $\text{cm}^3$  required to account for the observed infrared continuum absorption, is shown quite clearly. Thus, if ions are involved in the formation of water clusters responsible for the continuum absorption, they must necessarily play an intermediate role. The dashed curve indicates the number of ions which would theoretically be required to cluster "all" vapor molecules, based upon known ion to cluster ratios in real atmospheres. The small arrows in Figure 17 indicate that cooling steam can contain enough ions to (theoretically) cluster

"all" water vapor in moist air at room temperature. Experimental data related to these speculations will be discussed in the following sections of this report.

#### 4. RESULTS

The results obtained in the theoretical and experimental investigations discussed in the previous sections will be presented below in the same sequence.

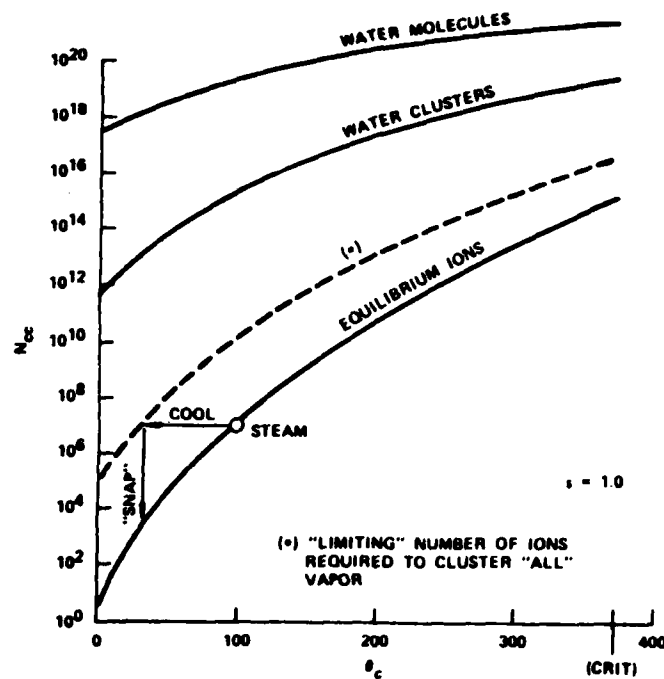


Figure 17. Numbers of Water Species Per  $\text{cm}^3$  ( $N_{cc}$ ) vs. Temperature for  $s = 1.0$ .

#### 4.1 Infrared Measurements.

The author's infrared radiometric studies of steam produced 3 kinds of evidence that water species other than the vapor (monomer) and droplets were present in warm water fogs.

1. For lower cloud densities, when the "effective emissivities",  $\epsilon_\lambda$ , of the fogs were less than 1.0, it was found (as found earlier by Carlon<sup>24</sup>) that the emissivities were much

larger than could be accounted for by simple vapor/droplet models.

2. For higher cloud densities, values of  $\epsilon_\lambda > 1.0$  were observed like those of the "phase transition luminescence" described by Potter and Hoffman<sup>29</sup> and attributed by them to water clusters of sizes  $c = 11$  and  $c = 17$  molecules per cluster.

3. In the emission spectra, features like "bumps" were observed which were similar to those observed earlier by Varanasi et al.,<sup>8</sup> in measurements of the infrared continuum absorption; these workers had concluded on other grounds that their results were consistent with the idea of hydrogen bonding as a contributor to the infrared absorption coefficient of water "vapor".

The effective (mean) liquid droplet diameters of steam-generated water fogs were known in these measurements,<sup>35</sup> and extensive Mie calculations<sup>58</sup> of the scattering and absorption components of fog droplets at the  $10 \mu\text{m}$  wavelength had previously been performed.<sup>26</sup> Thus, we determined with a high degree of confidence the contribution to total observed emission at the  $10 \mu\text{m}$  wavelength, and at adjoining wavelengths, predicted from simple droplet models and, by difference, determined the level of anomalous emission since water vapor is not a significant contributor in the 7-13  $\mu\text{m}$  atmospheric "window" region.

Three sources of modulated radiation, identified earlier, could reach the radiometer detector and contribute to the emissivity of a steam cloud. Since radiometric null existed in these trials ( $\theta_B \approx \theta_b$ ), there was no contribution to total signal by blackbody BB (Figure 7). At a cloud droplet mass concentration of  $C_D = 0.3$  to  $0.4 \text{ g/m}^3$ , when many of the most interesting examples of anomalous (Type "A") emission were observed, the probability of a single scattering event was only 0.16, of two events 0.026, and so forth. If the steel chamber wall emissivity  $\epsilon_w$  were appreciable (it is not about 0.1-0.2 for various stainless steels), or if the all temperature  $\theta_w$  were large compared to  $\theta_b$  (it was not - see Figure 8), a significant scattering contribution to total signal might have been expected. It was found that only direct emission from the cloud droplets themselves (for example, point B in Figure 7) was an important contributor to cloud emissivity of other water species (clusters) in the steam chamber were ignored.

Wolfe<sup>61</sup> gives a simple theoretical equation for the emissivity of a partially transparent body or volume acting as a distributed radiator. The equation can be written for a cloud of water droplets as:

$$\epsilon_{A_\lambda} = 1 - \exp(-a_{A_\lambda} CL) \quad (30)$$

where at wavelength  $\lambda$ ,  $\epsilon_A$  is the emissivity of the droplets themselves,  $a_A$  is the absorption component of the droplet mass extinction coefficient,  $m^2/g$ , obtained from the Mie calculations, and CL has already been mentioned as the product of droplet mass concentration in the cloud times path length, having combined units of  $g/m^2$ .

Figure 18 shows the values of  $a_A$  at  $\lambda = 10 \mu m$  from the Mie theory for spherical water droplets. Note that  $a_A$  is quite independent of droplet size distribution at this wavelength. Also shown in Figure 18 are the scattering coefficients,  $a_s$ , calculated for fog droplets, and the total extinction coefficient,  $a_T$ , which is the sum of the absorption and scattering coefficients.

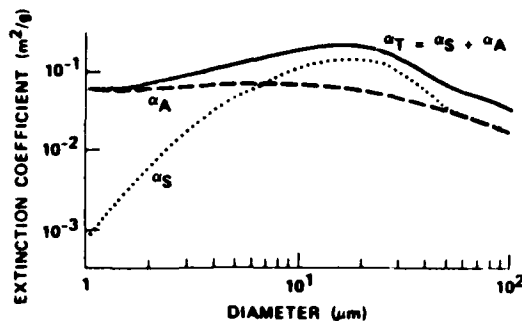


Figure 18. Curves Computed From the Mie Theory for Water Droplet Clouds, Showing Total Extinction Coefficient (Solid Curve) with Absorption (Dashed Curve) and Scattering (Dotted Curve) Contributions, as Functions of Droplet Diameter; Wavelength =  $10 \mu m$ .

The data will show that the emissivity values obtained from warm fogs were 5 to 10 times larger than could be explained by droplets or vapor (monomer) in the test chamber. If it were possible somehow to explain this anomaly by a combination of more elaborate cloud models and manipulation of the experimental data, one would still have to address the luminescencelike activity shown by the points lying above the 1.0 ordinate value in the following curves, and the pronounced spectral activity which is apparent in these curves.

In the figures to be discussed, the ordinate is the "apparent emissivity",  $\epsilon_\lambda$ , and the observation wavelength is shown as the abscissa. Concentrations of cloud droplets,  $C_D$ , are shown on the curves, as are the ranges of cloud temperatures (Figure 8) over which the observations were made,  $\theta_c$ . The vertical "error bars" extended over one deviation of the data for several spectra averaged within a given droplet mass concentration and temperature range. Hence, one curve may

average from two to as many as seven separate spectra, which are grouped together because they have similar shape. The droplet mass (volume) concentration,  $C_D$ , could always be conveniently measured in the experiments, and thus gives a meaningful reference for these spectral observations.

Figure 19 averages four spectra from 28 observations. Examining this curve by itself, one would conclude that it shows "expected" near-blackbody behavior of the dense, opaque water cloud with a peak emissivity of 1.05 near  $\lambda = 10 \mu\text{m}$  (compared to 1.0 for a blackbody) being indicative of the magnitude of measurement error.

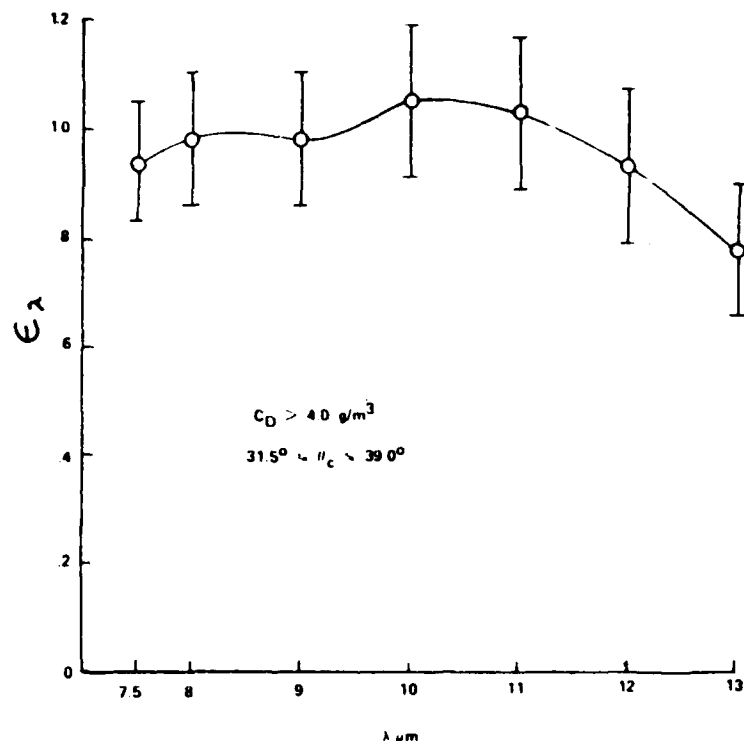


Figure 19. Emissivity Spectrum, Opaque Cloud Cooling From 39.0 - 31.5 °C, 28 Observations.

However, as the cloud cools slightly, the emission spectrum retains a similar shape but increases in intensity. This is shown by the upper curve of Figure 20, which includes 18 observations. The interpretation of this result appears to be that radiation produced by a mechanism responsible for cluster "luminescence" is, in turn, extinguished by absorption and scattering of the cloud droplets. But as the cloud becomes thinner, a maximum "luminescence" is obtained corresponding to the threshold of opacity of the cloud. This behavior was

observed when the transmission of the cloud was 1-2% at shorter wavelengths.

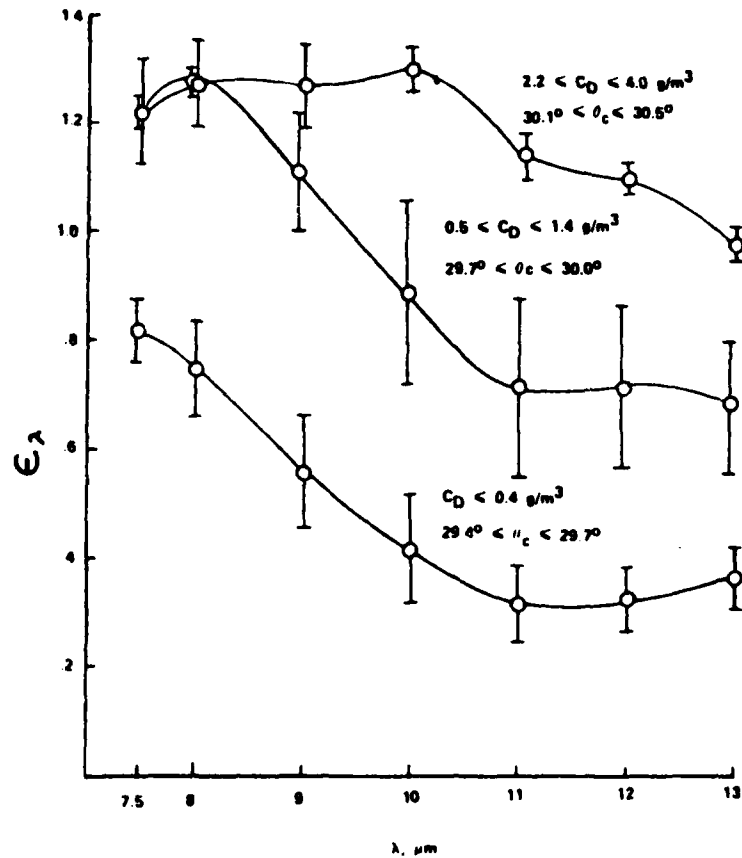


Figure 20. Emissivity Spectra, Cloud Cooling From 30.5-29.4 °C, 71 Observations.

As slight cooling and cloud droplet depletion continues (middle curve, Figure 20, 34 observations), an abrupt change in the spectrum occurs. The peak emissivity remains about the same near  $\lambda = 8 \mu\text{m}$ , but the curve becomes concave upward and the emissivity near  $\lambda = 10 \mu\text{m}$  falls below 1.0. Then, as cooling progresses (lower curve, Figure 20, 19 observations), the effect is as if the spectrum has shifted to shorter wavelengths, and all values lie below  $\epsilon_{\lambda} = 1.0$ . Taken by itself, this lower curve would not seem unusual. However, it is found that when measured droplet and water vapor concentrations are used to calculate their contribution to total cloud emissivity, the result falls far short of observation if simple models like Equation 1 are used. A discrepancy of 5-10 times is typical, depending upon wavelength.

Large changes in cloud temperature also result in significant changes in the emission spectra. In Figure 21, the curve of Figure 19 (mean  $\theta_c = 35.3^\circ\text{C}$ ) is compared to a spectrum for another cloud at  $\theta_c = 52^\circ\text{C}$  (18 observations), where both clouds were in the same range of droplet mass concentration,  $C_D$ .

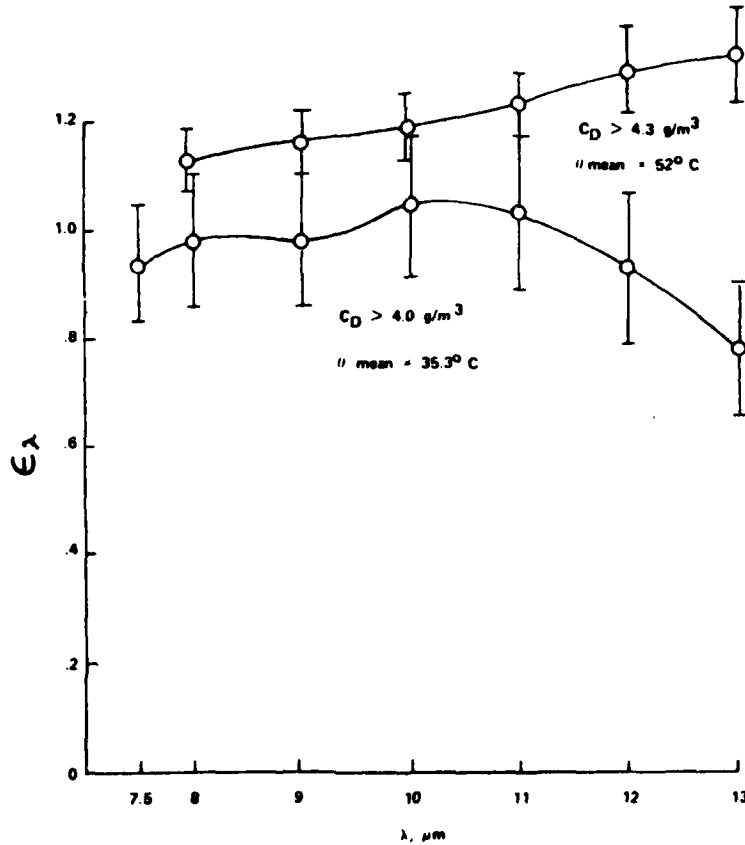


Figure 21. Emissivity Spectrum of Figure 19 Compared to Spectrum for Opaque Cloud at  $52.0^\circ\text{C}$ , 18 Observations.

The curve for the warmer cloud lies above that for the cooler one. However, recalling that dense clouds exhibit an emissivity saturation effect at highest droplet mass concentrations, it is observed in Figure 22 that, as  $C_D$  falls, the higher-temperature spectrum (18 observations) now lies below the curve for a comparable, cooler cloud (upper curve, redrawn here from Figure 20, for comparison). This suggests that, whatever cluster species might be present, the numbers of intermolecular hydrogen bonds might be present, and the numbers of intermolecular hydrogen bonds responsible for the intensity of spectral absorption would

be fewer at higher temperatures than at lower ones. This would imply that the mean cluster size,  $c_{\mu}$ , should have a negative temperature dependency. The changes in spectral shapes also suggests that the cluster distributions are changing, and the spectral "bumps" are like those of Varanasi et al.,<sup>8</sup> but at somewhat different wavelengths.

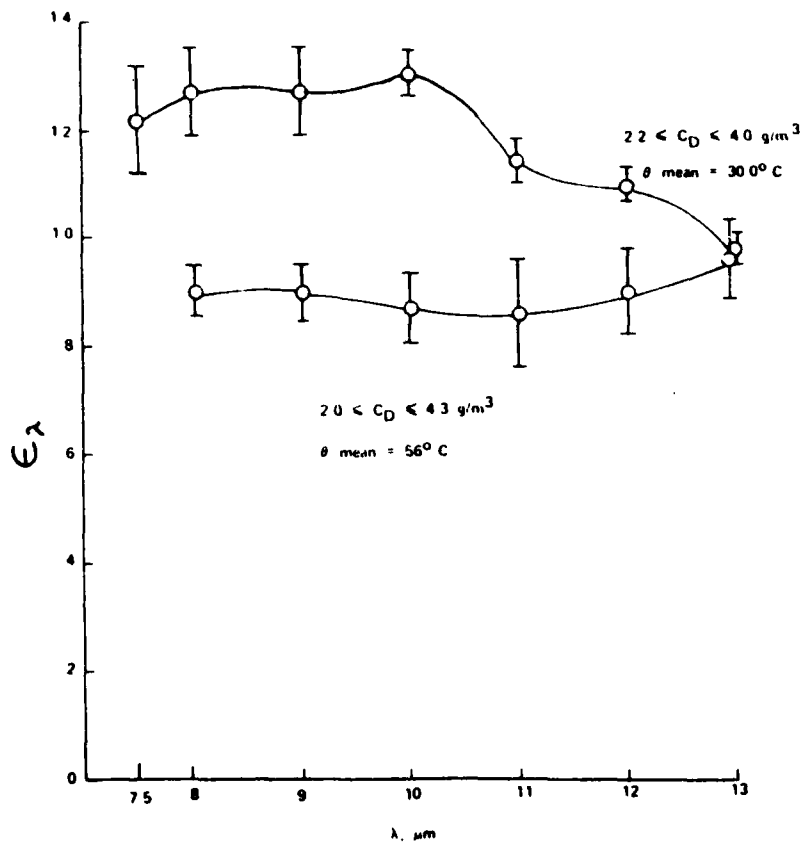


Figure 22. Emissivity Spectrum of Upper Curve, Figure 20, Compared to Spectrum of Cooling Cloud at  $56^\circ\text{C}$ , 18 Observations.

In Figures 23 and 24, the remaining curves of Figure 20 for lower  $C_D$ 's near  $30^\circ\text{C}$  are compared to spectra for similar droplet mass concentrations at a mean cloud temperature of  $\theta = 52^\circ\text{C}$  (18 observations and 14 observations, respectively). In Figure 24, the curve shapes are nearly the same, suggesting that, whatever their mean sizes and concentrations, the cluster species present when  $C_D \leq 0.4 \text{ g/m}^3$  are at least similar at both temperatures.

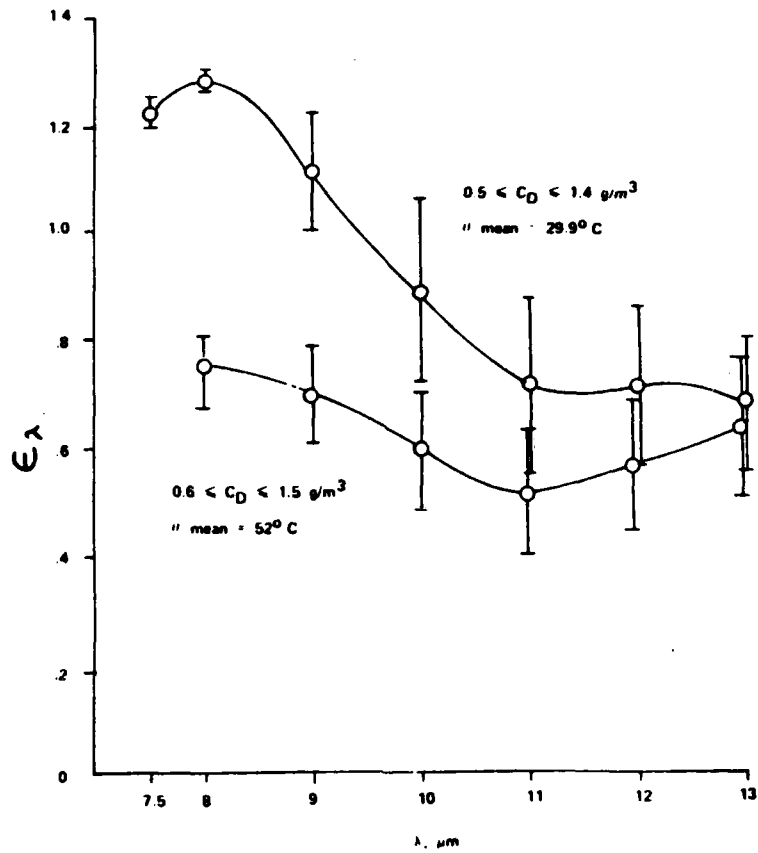


Figure 23. Emissivity Spectrum, Middle Curve Figure 20, Compared to Spectrum of Cooling Cloud at 52 °C, 18 Observations.

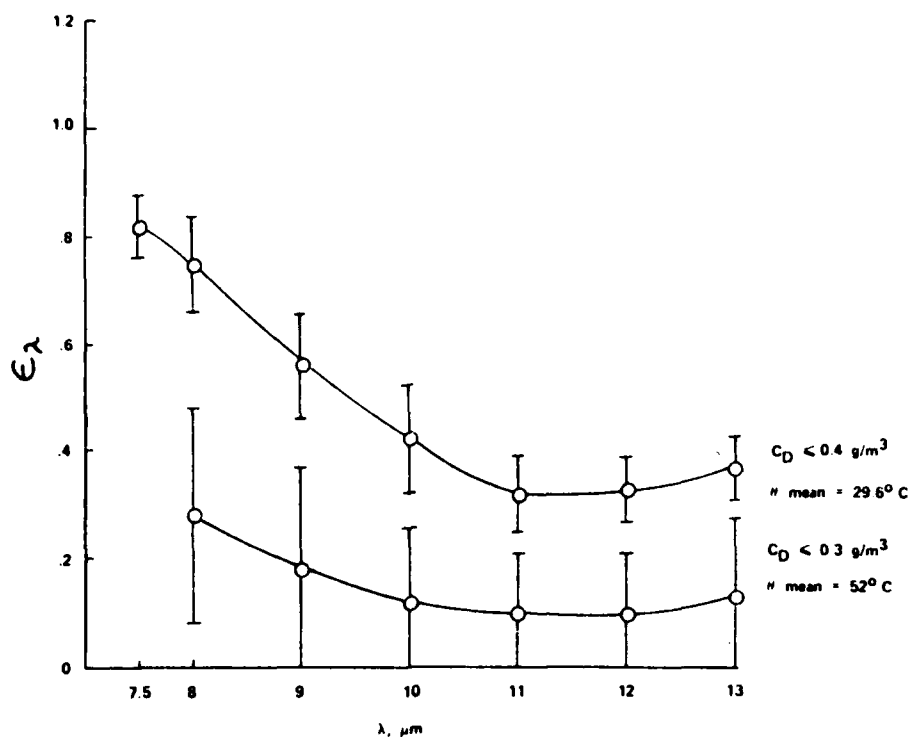


Figure 24. Emissivity Spectrum, Lower Curve Figure 20, Compared to Spectrum of Cooling Cloud at 52 °C, 14 Observations.

In some experiments, after a cool-down period of 40-50 min (Figure 8), there occurred a sudden loss of the anomalous emission signal. Within 20-30 sec, the emissivity of these samples fell from the levels shown in the curves to levels which could be explained by the concentrations of water droplets remaining in the chamber (using a small vapor correction). Apparently this signal loss corresponds to a sudden reduction or redistribution in the numbers of cluster species, perhaps corresponding to the loss of saturation humidity. It will be shown that steam has a very high ionic content, as shown by the "steam" point in Figure 17. The evidence suggests that ion-induced water clusters do not rapidly disintegrate in saturated water vapor, but that their populations can be sustained for periods at least approaching an hour. Thus, as the steam samples cooled in these experiments, artificially-high

populations of clusters must have been maintained at temperatures much lower than the normal equilibrium ones. This cooling, followed by the sudden loss of the surplus population (a phenomenon nicknamed "snap" by the author, as shown on the vertical arrow in Figure 17), would have accounted for the observation of anomalous emission signals over a chamber path length of 3.05 m, which normally can only be observed over atmospheric optical paths of hundreds of meters. There is infrared spectral evidence that steam-generated water vapor contains greatly-enhanced water cluster populations. This would seem to substantiate the observation of Elsasser<sup>1</sup> that the continuum absorption, which could not be seen in water vapor at room temperature, could be studied in steam. But, it would also seem to underscore the author's contention that Elsasser may have modeled clusters, not monomers, while explaining them by empirical extensions to monomer theory.

#### 4.2 Electrical Conductivity Measurements.

The author's measurements of electrical conductivity in moist air, which were made using the conductivity cells shown in Plates 1 and 2, gave results which seemed to be consistent with his infrared radiometric measurements. Typical behavior of the resistance of the large sample cell with humidification is shown in Figure 25. The dashed curve indicates the small (compensating) cell whose resistance is determined almost exclusively by insulator leakage. The solid curve represents the resistance measured for the moist air (only) between the large cell plates. This curve is obtained by correcting the actual resistance of the large cell for the leakage of the insulators as indicated by the compensating cell (with an identical insulator configuration). Thus, the dashed curve can be thought of as representing ions on the insulators, while the solid curve can be thought of as representing the ions in the moist air sample. Further details of the measurements have been reported in Carlon's "Ion Content and infrared Absorption of Moist Atmospheres," and elsewhere.<sup>60,61,62</sup> Note that at the beginning of these particular trials (upper ends of the curves in Figure 25), the leakages of the insulators dictated their resistances of both cells (about  $3 \times 10^{10}$  ohms). But as slow steam humidification progressed, the "leakage" of the moist air rapidly overtook the insulator leakage as the major contributor to overall leakage, or lowered resistance, of the large cell.

After humidification, the cabinet steam sampling slit was closed to exclude additional water vapor. In this experiment, the hot plate was used to increase the temperature of the moist air sample in the compartment from 29 °C to about 62 °C. This decreased the saturation ratio "s", as shown on the abscissa of Figure 25, from a value near saturation to  $s = 0.3$ . The measured resistance of both cells remained about the same, indicating that the numbers of ions did not change appreciably. The moist air sample was then allowed to cool, as shown by the upper parts of the "loops" in the curves of Figure 25. By the

completion of the experiment, which in this case lasted for 3 hrs and 39 min, the insulators had become sufficiently saturated with moisture to bring their resistance down to a level close to that of the residual moist air between the large cell plates.

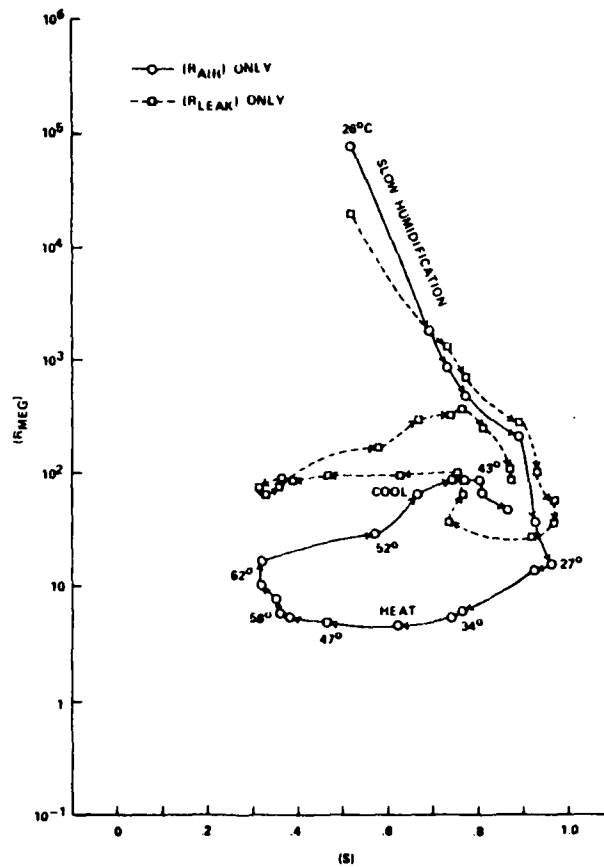


Figure 25. Cell Resistance vs. Humidification by Steam Generated Water Vapor. The Dashed Curve Shows Insulator Leakage Resistance for Either Cell (Representing Ions on the Insulators), and the Solid Curve, by Difference, Shows the Resistance Due Only to Moist Air Between the Large Cell Plates (Representing Ions in the Moist Air).

Another way to look at the data of Figure 25 is to convert the moist air resistances to ion concentrations by using Equation 9. The result is shown in Figure 26. At the beginning of the experiment, the air sample in the box contained about 300 ions per  $\text{cm}^3$ . This result agrees well with expected values. However, as the air was humidified by water vapor generated by boiling, the ion count increased very rapidly to a level in excess of  $N = 10^6$  per  $\text{cm}^3$ . This ion concentration was maintained, and even slightly enhanced, as the moist air sample was heated. Since these measurements were made in stagnant (not flowing) air, this implies that an ion regeneration mechanism maintained rather stable populations for periods of up to an hour or more. Finally, when the sample compartment was vented to room air and the moist air sample was allowed to cool,  $N$  began to return to normal. The peak value of  $N$  reached in this experiment, in which ions were generated by boiling water, namely  $10^7$  per  $\text{cm}^3$ , is in agreement with this same value shown for steam at  $100^\circ\text{C}$  in Figure 17, on the curve labeled "equilibrium ions".

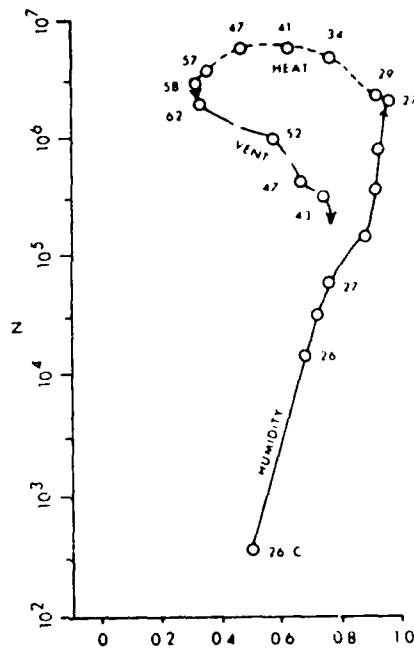


Figure 26.  $N$ , Number of Ions Per  $\text{cm}^3$  of Moist Air vs. " $s$ ", the Saturation Ratio or Fractional Relative Humidity; Celsius Air Temperatures Are Shown for Most Experimental Points.

The results reported here were obtained under conditions which differ from those of usual conductivity measurements in at least two respects: (1) the air samples were allowed to equilibrate between the cell plates and not flow rapidly through the cell; and (2) a very sensitive cell was used, for which the insulator leakage as a contributor to measured resistance was accurately known under all conditions. Thus, the results cannot be compared directly to those of conventional measurements of atmospheric ion concentrations. They suggest that an incomplete understanding exists of the hydrated ions present in moist air and of their dependency upon the means by which they are generated. Apparently steam contains large numbers of ions which may be present simply because of the strong positive temperature dependency of the dissociative ion product of water (Equations 6).

If self-dissociation of water vapor were a significant source of ions at, say, 27 °C, this contribution at 100 °C from Equation 6 would be about 100-fold larger in water vapor over boiling water than in normal ambient, saturated air. But this would account for only 2 of the 4 orders of magnitude change shown in Figure 26. It is known that newly-formed ions in water vapor are swarmed by water molecules and are hydrated in less than a microsecond.<sup>49</sup> Thus, these species would almost certainly be small, singly-charged, hydrated ions of the mobilities (1-2 cm<sup>2</sup>/volt-sec) assumed in this report.<sup>40,41</sup> Blanchard<sup>63</sup> has shown that ions can be generated by bursting bubbles which are sure to be present at the surface of boiling water, but the magnitude of this effect is less than that necessary to explain the results under discussion in the present work. Possibly, evaporation of tiny droplets torn loose from the surface of boiling water also contributes to the ion concentrations. Together, these 3 effects might explain the observed initial ion concentrations.

The apparent regeneration of the ions measured by the author also raises questions, especially since the moist air samples were stagnant while the ions were continually being drawn to the cell plates as the cell currents were measured. These measurements were carried out in a normal laboratory environment. No high-powered, electro-magnetic sources or other unusual ion generation sources were present. When the moist air sample was vented to room air, the ion count fell rapidly to normal laboratory levels. Ordinarily, results such as those observed here would suggest that electrode leakage had accounted for this behavior. But, this seems extremely unlikely in view of the precautions taken, the techniques used, and the reproducibility observed in these measurements as has been discussed previously. Therefore, the results suggest new findings which are not yet explained by theory.

Support for a theory of ion regeneration in steam-humidified air can be found in the infrared measurements. There is considerable evidence that ion hydrates and the hydrogen-

bonded clusters of molecules which remain after charge neutralization, are strong contributors to the infrared continuum absorption of water vapor. Water vapor generated by boiling or by the direct use of saturated or superheated steam is known to produce extremely strong infrared absorption, attributable to modes of ion hydrates or neutral water clusters having an average of about 10 water molecules per cluster.<sup>52</sup>

Infrared measurements indicate that the number of clusters per  $\text{cm}^3$  is about  $10^{13}$  -  $10^{14}$  in steam-generated, saturated water vapor at 100 °C. Small ions (ion hydrates) are thought to be essential in the process, wherein intermolecular hydrogen bonds "cross-link" the water molecules clustered about each ion leaving behind tiny, stable, latticelike water clusters which can survive in water vapor for an hour or more after the loss of the ionic charge. The numbers of clusters, and hence the strength of their infrared absorption, have been found to be directly proportional to the ion product of water (Equation 5). Hence, from the ion product it is calculated that the numbers of positive or negative ions in saturated water vapor at 100 °C should be about  $10^7$  -  $10^8$  per  $\text{cm}^3$ . This result is in good agreement with values near  $10^7$  per  $\text{cm}^3$  reported in the present work for air humidified by boiling water. Furthermore, since the populations of neutral clusters exceed the populations of ions by about  $10^7$  per  $\text{cm}^3$ , it is clear that simple equilibria could continue to provide replacement ions under experimental conditions, such as those reported here, for many hours. This ion regeneration hypothesis, based upon the independent body of infrared research data, seems completely consistent with the result reported in the present report.

The conductivity results, including those from the studies of insulator leakage, indicate that the conductivity of moist air might be a more important factor than was previously realized in space charge dissipation. Presently, it is believed<sup>64</sup> that insulator leakage effects, rather than moist air conductivity, can explain certain phenomena, for example, the well-known humidity dependence of annoying static-electric shocks received by persons moving and touching objects in dry, heated rooms in winter. In fact, some of the new data suggest that the electrical conductivity of moist air has a quadratic, or even a cubic, dependency upon its saturation ratio. One might also consider possible physiological effects due, for example, to high ion concentrations generated by boiling water room humidifiers.

#### 4.3 Simple Cluster Models.

Figure 27 shows the infrared continuum absorption spectrum actually measured in superheated steam at 400 °K by Varanasi et al.<sup>8</sup> Similar results have been obtained by the present author in the measurements of saturated steam at 373 °K, by Varanasi et al., but they show similar "bumps" or small bands

in the spectra. For example, in Figure 20, small bands are seen near 8  $\mu\text{m}$  and 10  $\mu\text{m}$ .

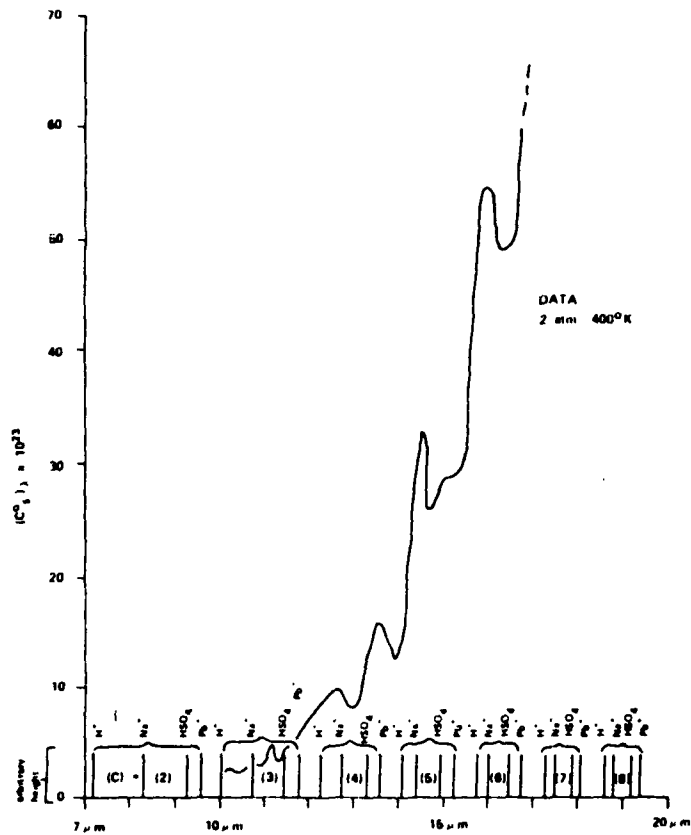


Figure 27. Spectrum of Superheated Steam (400 K)  
Obtained by Varanasi et al.<sup>8</sup>

It is found that most of the small bands shown in Figure 27 are spaced in such a way that they can be assigned an integer if (and only if) there exists an empirical relationship or progression with a constant of 6.4, such that:

$$\lambda_c = 6.4 \sqrt{n} \quad (31)$$

where "n" is the integer. But, this is precisely the form of the derived Equation 18, for  $n = c$  and  $K'' = 6.4$ . Thus, the spacing

of the small bands in Figure 27 suggests that if an absorption line was associated with each cluster of a given size and geometry, and if these clusters were distributed in water vapor, that the continuum absorption might be considered to be the envelope of absorption lines associated with these statistical distributions of discrete cluster sizes. Only those lines corresponding to the most energetic modes would appear in this wavelength region. For example, the homogeneous dimer ( $c = 2$ ) has 6 interatomic and 6 intermolecular (cluster) modes,<sup>15</sup> only one of which is found in this high-frequency (short wavelength) region. Other studies of water clusters ranging in size from the dimer to the pentamer ( $c = 5$ ) have identified no lines at wavelengths shorter than about  $13.9 \mu\text{m}$ ,<sup>18</sup> assuming known bond energies. Therefore, it is likely that the small bands discussed here are observable in this wavelength region because few other cluster modes are spectrally active in this region. This is probably the reason that such a simple oscillator model seems to work in this region. From these data, it should be possible to construct a cluster distribution which could account for the observations. This will now be considered.

The rectangles of arbitrary height drawn along the abscissa of Figure 27 (bracketed groups of lines) represent the spread of values of  $\lambda_c$  calculated from Equation 14 for ion masses,  $m$ , ranging from 1 ( $\text{H}^+$ ) to 207 ( $\text{Pb}^+$ ), with arbitrarily-chosen lines for other species shown in between ( $\text{HSO}_4^-$  and  $\text{Na}^+$ , for the latter of which  $m \approx M$ ). The left-hand rectangle is for an ion-induced cluster of size ( $c$ ) = 2, and the right-hand rectangle is for ( $c$ ) = 8. Note that as "c" increases in Figure 27, "m" becomes a smaller fraction of the total cluster mass (Equation 13) and the spread of spectral lines narrows for the simple oscillator model. Thus, the bands of lines associated with each cluster size "sharpen" toward higher c's or longer wavelengths, and the resonances associated with each cluster species become spectrally more clearly defined. But at shorter wavelengths where the rectangles in Figure 27 are very broad, the measured infrared continuum absorption should depend heavily upon the numbers and kinds of ions present, since the line locations are very dependent upon  $m$ , the ion mass. Measurements taken in the  $7\text{-}10 \mu\text{m}$  wavelength region are highly variable and difficult to reproduce. This is seen in the author's measurements (Figures 19 - 24) and in the spread of experimental data points commonly found even in the most carefully-controlled transmission (absorption) measurements in this wavelength region (open circles, Figure 11).

If the continuum absorption is due to modes of bonds in statistical distributions of vapor-phase water clusters, then infrared spectra of the continuum should give clues as to the shape of these distributions. Equations 18 and 31 have already given an indication that a simple relationship exists between the line wavelength and size,  $c$ , of the cluster species responsible for this absorption. Carlon<sup>49,65</sup> has argued that the cluster species producing these regularly-spaced absorption

lines should be symmetrical or closed-ring structures. From these observations, and the assumption of a symmetrical distribution, it is possible to construct a graphical representation of the distributions of water clusters, by size "c", which theoretically should exist in water vapor or in moist air. Two such curves are shown in Figure 28, where the lower curve is for saturated water vapor ( $s = 1.0$ ) and the upper curve is for supersaturated water vapor ( $s = 4.2$ ), both at 23 °C. The "critical" supersaturation occurs near  $s = 4.2$ , as shown by the peak in the "ion" curve of Figure 6. The curves suggest that droplets will form at the critical size for nucleation (arbitrarily shown as  $c = 30$  in Figure 28) when the upper "tail" of the water cluster distribution contains at least a few clusters of this size at  $s = 4.2$ . The ordinate scale of Figure 28 shows the mass fraction of total water vapor which is bound into clusters of each size, under the conditions shown. The abscissa also could be calibrated in wavelength,  $\lambda_c$ , using Equation 31 for  $n = c$ , in which case the lower c "tails" of the curves would resemble infrared spectra of these cluster distributions in water vapor (Figure 27), where the envelope of the spectrum appears to be "draped" over the absorption lines of clusters having some discrete distribution. Using similar computational techniques, the cluster number distribution also can be inferred. This is shown in Figure 29, where a contribution is included for the homogeneous dimer and trimer as a reminder that these cluster species may play a role (perhaps as significant role) in the infrared continuum absorption.

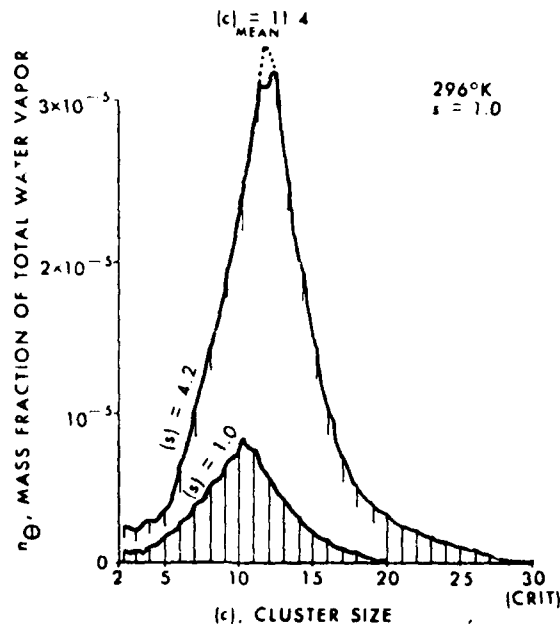


Figure 28. Distributions Showing Calculated Mass Fractions of Total Water Vapor which Are Bound into Clusters of Each Size (c) at 23 °C.

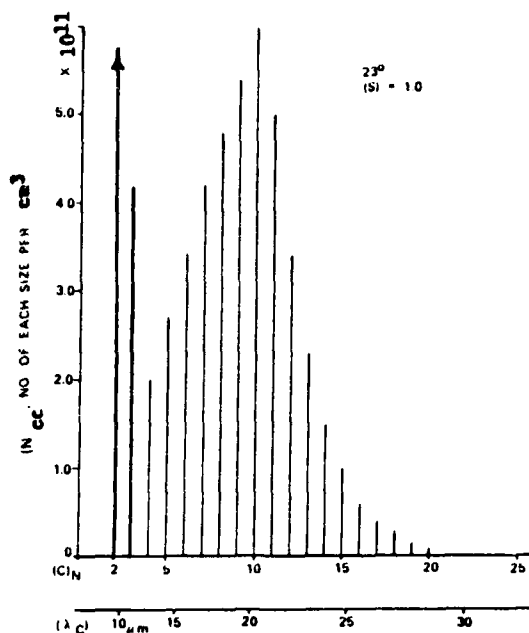


Figure 29. Cluster Number Distribution.  $\lambda_c$  Is also Shown, from Equation 31 for  $n = c$ .

#### 4.4 The Thermodynamics of Clustering.

Carlson<sup>31</sup> has discussed the work of himself, Gebbie, and others, which shows that the anomalous absorption in the atmosphere at low temperatures cannot be attributed to water dimers in equilibrium. Varanasi et al.<sup>8</sup> first gave evidence that the dimer was a candidate to explain the infrared continuum absorption from the standpoint of temperature dependency. It was assumed that a Boltzmannlike distribution of neutral clusters would exist in water vapor as is shown for the largest estimated cluster populations in Figure 30.

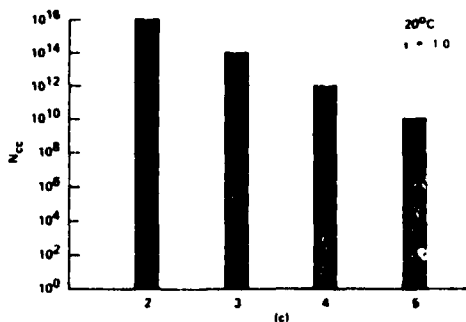


Figure 30. Number Distribution of Homogeneous Clusters.

McDonald<sup>65,66</sup> gave the form of this distribution as:

$$(N_c)_N = N_1 \exp (-\Delta F/k\theta) \quad (32)$$

where  $(N_c)_N$  is the number of clusters of size "c" per unit volume,  $N_1$  is the number of monomers per unit volume,  $\Delta F$  is the free energy of cluster formation,  $k$  is Boltzmann's constant and  $\theta$  is the absolute temperature. Abraham<sup>67</sup> has given a detailed discussion of homogeneous nucleation and estimates of homogeneous cluster populations under conditions such as those found in real atmospheres. While these populations might be large enough to account for observed levels of absorption under some conditions, they do not seem applicable at higher temperatures.

Figure 31 shows a plot (upper, solid curve) of Equation 24, which was derived earlier in this report. The form of this curve agrees reasonably well with the plotted data of Montgomery,<sup>68</sup> who found that at higher temperatures the continuum absorption coefficient  $(C_c^0)_\lambda$  in the  $8 \mu\text{m}$  wavelength region, reaches a minimum and then begins to increase again. Earlier measurements had included only that range of temperatures below  $115^\circ\text{C}$  represented by the left hand portion of the curves in the figure. Thus, empirically-obtained temperature corrections, such as that of Roberts et al.,<sup>33</sup> approximated the slope of the curves for earlier data (their curve is shown dashed in Figure 31). For comparison, Figure 31 also shows two curves (square and triangular points) for Boltzmannlike temperature dependencies (Equation 32), where cluster formation energies are expressed as "binding energies",  $B$ , in electron volts; these curves would represent predicted temperature dependencies if the homogeneous dimer were responsible for the continuum absorption. The figure indicates that the dimer explanation leads to incorrect predictions at higher temperatures and, by inference, is incorrect based upon experimental results at elevated temperatures. The upper curve (Equation 24) agrees much more closely with the experimental results because of the change in  $\Delta H$  with temperature. This equation was derived using the assumption that intermolecular (hydrogen) bonds in water clusters responsible for the infrared vapor continuum absorption are at least similar to bonds found in bulk liquid water.

The sheer numbers of water clusters which are necessary to explain the infrared continuum absorption seem, at first thought, to be prohibitive. Figure 17 shows that about  $10^{12}$  clusters per  $\text{cm}^3$  would be required at  $0^\circ\text{C}$  in saturated air ( $s = 1.0$ ). But even in his first cloud-chamber work, C. T. R. Wilson<sup>69</sup> estimated that  $10^8$  clusters per  $\text{cm}^3$  were present in the "cloudlike" condensation which he attributed to neutral clusters always present in water vapor. Wilson's estimates were based on normal ambient starting conditions, using vapor saturated air. He also found less than 100 ions per  $\text{cm}^3$  which produced

"rainlike" condensation at lower supersaturations ( $s = 4.2$ ; see "ion" curve, Figure 6). This agrees with the ion population at 0 °C shown in Figure 17. Wilson also found bright color "tints" and other evidence which suggested that the droplets grown from clusters had peaked distributions with well defined maxima.

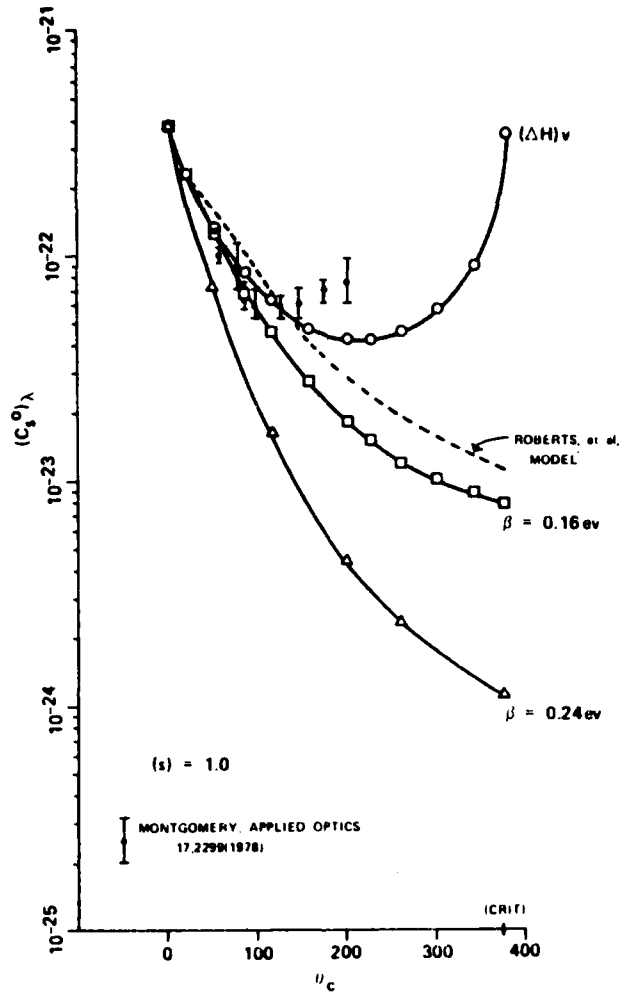


Figure 31. Variation of the Continuum Absorption Coefficient with Temperature; Several Modeling Equations are Compared with the Recent Data of Montgomery.<sup>68</sup>

Wilson based his  $10^8$  per  $\text{cm}^3$  figure upon observations of the clouds produced using light scattering from a gas flame. It is likely then that he would not have been able to see more than  $10^8$ - $10^9$  droplets grown from clusters per  $\text{cm}^3$  because of natural limits which exist on the detection of droplets using condensation techniques. Even the modern laser illumination and minimum detectable droplet diameters as small as  $0.1 \mu\text{m}$  in the optical

wavelengths, the optical limit of detection only approaches  $10^{10}$  per  $\text{cm}^3$ . This can be easily demonstrated by a simple derivation using the gas laws and elemental geometry to find that the limiting number of water droplets that can be grown using all of the water vapor in a  $\text{cm}^3$  is:

$$(N_{cc})_{lim} = \frac{5.5 \times 10^8 (s) (p_0)}{\theta_k \rho D_\mu^3} \quad (33)$$

where  $(N_{cc})_{lim}$  is the number,  $(s)$  is the saturation ratio,  $(p_0)$  is the saturation vapor pressure at temperature  $\theta_k$  ( $^\circ\text{K}$ ),  $\rho$  is the mass density of the individual droplets,  $\text{g}/\text{cm}^3$ , and  $D_\mu$  is the geometric mean droplet diameter,  $\mu\text{m}$ . If it is assumed that the starting conditions for a condensation operation are saturated air at  $20^\circ\text{C}$ , it can be calculated that about  $10^{10}$  droplets might be detected per  $\text{cm}^3$  if droplets as small as  $0.1\mu\text{m}$  could be resolved by scattered light.

In summary, from Wilson's results<sup>69,70</sup> it can be inferred:

- Wilson's electrically-neutral nuclei for "cloudlike" precipitation and the species responsible for the infrared continuum absorption are one and the same - that is, neutral water clusters.

- The numbers of neutral clusters (for example,  $10^{12}$  or less per  $\text{cm}^3$  at  $0^\circ\text{C}$ ) necessary to account for the infrared continuum absorption may, in fact, exist in moist air but may not be measurable using optical light-scattering techniques.

Wilson also found that moist hydrogen gas was peculiar in its behavior when he attempted to precipitate clouds in it as he had done in air and in other gases. Hydrogen frequently would not produce droplets upon expansion when moistened. There may be a connection between this result and recent work hypothesizing that neutral cluster formation via dissociative ions of water itself, including  $\text{H}^+$  as  $\text{H}_3\text{O}^+$ , is an important mechanism in explaining the anomalous absorption and emission of water in the infrared, especially at elevated temperatures as in steam.

## 5. DISCUSSION

Many kinds of evidence has been presented in this report showing that water vapor contains statistical distributions of intermolecularly-bonded, probably ion-induced, water clusters of discrete sizes and geometries. Equations can be derived from thermodynamic theory, which allows mean cluster sizes to be understood as functions of temperature and humidity. Consistency has been demonstrated between the properties of

hydrogen-bonded water molecules in the liquid-phase and those in vapor-phase clusters. Consistency of behavior has been demonstrated not only near typical ambient temperatures, where great differences exist between the vapor and liquid phases of water, but also at temperatures up to and including the critical. Discussions have linked ions and cluster species, which are well known to cloud physicists and researchers in atmospheric electricity, to new experimental data on anomalous absorption of the atmosphere, infrared steam emission spectra, and electrical conductivity in steam.

In describing the methodology of this work, several hypotheses were set forth which were to be tested by experiment (or observation) in an attempt to find a solution to the problem of anomalous infrared absorption by molecular clusters in water vapor. These hypotheses will now be considered in light of the findings presented in this report:

a. "Water vapor contains complexes or 'clusters' of water molecules which are phase-transitional species between the vapor and liquid phases. They cannot be observed directly by any known experimental techniques." While it is true that water clusters cannot be observed directly by known techniques, it is also true that the cloud chamber can give physical evidence for the existence of clusters which is nearly as satisfying as if direct observation were possible. As early as 1897, C. T. R. Wilson<sup>69</sup> had shown that ions and neutral clusters are present in water vapor, and that subcritical nuclei like these could be nucleated by supersaturation to produce droplets on a one-to-one basis. Within the limitations of his optical methods, Wilson was able to estimate that about  $10^8$  neutral clusters were "always" in each  $\text{cm}^3$  of water vapor near ambient conditions. It has been shown (Equation 33) that  $10^{11}$ - $10^{12}$  neutral clusters per  $\text{cm}^3$  (Figure 17) might, in fact, exist and that populations of this order could account for the infrared continuum absorption. Abraham<sup>67</sup> and others have shown that homogeneous nucleation theory can also predict cluster populations approaching these magnitudes. But several kinds of evidence exist suggesting that many types of cluster species (not just dimer, trimer, etc.) are present in huge numbers in water vapor.

For example, the temperature dependency of the infrared continuum absorption (data, Figure 31) is not consistent with homogeneous cluster theory. The proportionality of the ion product of water with temperature to the continuum absorption coefficient with temperature (Equation 5) might be fortuitous or significant but, in either case, argues for ion-induced cluster species in water vapor. Infrared emission spectra (Figures 19-24) or transmission spectra (Figure 27) of steam exhibit small "bumps" or bands which appear or disappear with environmental changes in ways which are suggestive of distributions of clusters of many sizes in the vapor-phase. Luminescencelike behavior is also observed, which Potter and Hoffman<sup>29</sup> attributed

to clusters of at least 11 and 17 molecules in phase-transitional water. The small bands can be shown to be spaced in a wavelength with a dependency predicted even by the simplest cluster modes (Equation 14) and to become progressively sharper as the cluster size increases. The author's measurements have shown that conditions (for example, steam) which favor enhanced conductivity (ion count) in water vapor also favor enhanced, and proportional, anomalous absorption. Figure 6 (dotted curve, labeled "uncharged") indicates that truly neutral clusters in supersaturated water vapor should grow without limit into droplets. Yet, C. T. R. Wilson found swarms of neutral clusters "always" present, suggesting that ion-induced, hydrogen bonded species are also possible whose domain would be represented by a curve like the solid curve labeled "ion" in Figure 6 for  $s < 1.0$ , but which are externally neutral. Therefore, J. G. Wilson's<sup>27</sup> comment that Equation 4 is "clearly incomplete when, as for water, strongly polar molecules form an oriented surface layer" may be a very important one.

It is concluded, on the basis of the evidence presented here, that water vapor definitely contains complexes or "clusters" of water molecules which are phase-transitional species between the vapor and the liquid phases. Hence, Hypothesis 1 is correct.

b. "The modes of intermolecular or ion-molecular bonds in these clusters give rise to the anomalous infrared 'continuum' absorption and probably to similar phenomena at longer wavelengths as well. It should be possible to calculate infrared spectral lines or bands of these modes." A lengthy discussion has been presented concerning water vapor models and early empirical corrections to these models using data taken from steam. Extensive evidence has been presented here that steam contains rich concentrations of ions and of water clusters. Models ranging from the simplest oscillator to detailed, ab initio calculations for water clusters (i.e., Newton,<sup>37</sup> Owicki et al.<sup>16</sup>) have been developed, and it has been shown that bands or lines predicted for intermolecular modes of many kinds if clusters lie within the wavelength interval of the infrared continuum absorption. Furthermore, distributions of ion or ion-induced neutral clusters, like those considered in Figure 28, infer that the entire continuum absorption spectrum (Figures 11, 12, 27) is explicable as the envelope of all lines of modes contributed by all clusters of the statistical distributions of these species. These species happen to be present when a given water vapor absorption or emission measurement is made. Thus, all cluster advocates, whether they be dimerists or students of myriad cluster species in water vapor, explain the continuum absorption as being due to intermolecular modes of water molecules, and their combined evidence must be considered as contrary to the monomerists' view that simple empirical changes to traditional band or line models can explain the observations.

It is concluded that modes of intermolecular or ion-molecular bonds in cluster distributions can explain the continuum absorption, and similar observations of anomalous absorption in other wavelength regions. It is also concluded that spectral line or band positions can be calculated for these modes, and that there is ample evidence in the literature that calculations agree rather well with observations.

c. "The clusters form and exist in water vapor by mechanisms which are describable using classical thermodynamic and chemical bond theory, even though certain aspects of classical thermodynamics might be applicable on the molecular scale." Much evidence addressing this hypothesis was reviewed under Hypothesis a. Even in C. T. R. Wilson's earliest work,<sup>69,70</sup> he recognized that the nuclei responsible for this "rainlike" and "cloudlike" condensation were agglomerates (charged or uncharged) of relatively small numbers of water molecules. It is now clear that some misunderstanding existed as to the precise nature of these species, because classical thermodynamic treatments, which Wilson had to use, could not provide for small water clusters which were ion-induced (neutral), or hydrogen-bonded. The author's work reported here on electrical conductivity in water vapor suggests strongly that: (1) ions are essential to produce many kinds of neutral clusters (such as those neutral species responsible for Wilson's "cloudlike" condensation and numbering at least  $10^8$  per  $\text{cm}^3$ ); but (2) it is hydrogen-bonding that stabilizes these clusters, once formed, and gives them lifetimes comparatively enormous to those of the ionic charges; and (3) the ions are merely equilibrium species present with the much larger populations of neutral clusters, which are responsible for the continuum absorption.

It is concluded that these mechanisms are describable using classical theory, but that certain concepts, such as surface tension, must be discarded when dealing with clustering and nucleation on the molecular scale.

d. "Many atmospheric water species are involved simultaneously in mechanisms which were not previously recognized as being closely interrelated, for example, infrared absorption/emission, cloud droplet nucleation and electrical and electrostatic phenomena. Thus, there should be correlations between, for example, infrared absorption/emission and the electrical conductivity of water vapor or of moist air." The discussion in this report has served to focus attention upon two points which, although obvious, are overlooked by workers in specialized fields: (1) the same atmosphere is shared by infrared spectroscopists, cloud physicists, investigators of static electric phenomena, and meteorologists; (2) the same atmospheric species studied by infrared spectroscopists are also studied by spectroscopists at other wavelengths. Carlson<sup>32,31</sup> has summarized work by spectroscopists in many wavelength regions who report that, although its magnitude may vary, anomalous

absorption (with its characteristic temperature and partial pressure dependencies) is present in their spectral intervals. This suggests: (1) that if anomalous absorption is present at wavelengths much longer than infrared wavelengths, a monomer-rotational explanation may not be applicable, and (2) if it is not applicable there, it may not be applicable in the infrared either. Carlon<sup>32</sup> suggested a very simple test to predict whether anomalous absorption by water should be expected in a given wavelength region. The test consists of taking the ratio of absorption coefficients for liquid water to water vapor, wavelength-by-wavelength, and taking the magnitude of this ratio as indicative of clustering and spectral activity in water. The basis of the test is that liquid water is extensively hydrogen-bonded (clustered), while water vapor at normal ambient temperatures is not. Therefore, any absorption coefficient ratios (liquid to vapor) much larger than unity are evidence for clustering and spectral activity at the observation wavelength, especially if the ratio varies as the vapor partial pressure varies. The results of an investigation like this, through the radar region, are shown in Figure 32. The ratio  $> 10^4$  in the 10  $\mu\text{m}$  wavelength region stand out immediately. This is the region of the most intense infrared continuum absorption by water vapor. Smaller peaks are found at longer wavelengths beyond 1000 m, which correspond to regions where anomalous absorption also has been observed. Continuum absorption in the 3-5  $\mu\text{m}$  window region is also indicated in Figure 32. A second ordinate scale relates observed levels of anomalous absorption to expected monomer levels. It can be seen that an anomalous component 10 times larger than the monomer level is not uncommon in the 10  $\mu\text{m}$  region, as infrared steam emission measurements reported here have shown in which levels 5-10 times those expected were measured.

It is concluded that commonality and close interrelationships exist between atmospheric water species described and measured by cloud physicists, investigators of electrostatics, and absorption or emission spectroscopists in many wavelength regions. The numbers and kinds of these species can be described by techniques known to these disciplines. As these interrelationships are better understood, new technology should be suggested or given a firmer theoretical basis. For example, infrared cloud chambers might be used to study pre-nucleation events. Or, a firmer basis for clear-air-turbulence (CAT) detection ahead of aircraft<sup>21</sup> might emerge from cluster theory.

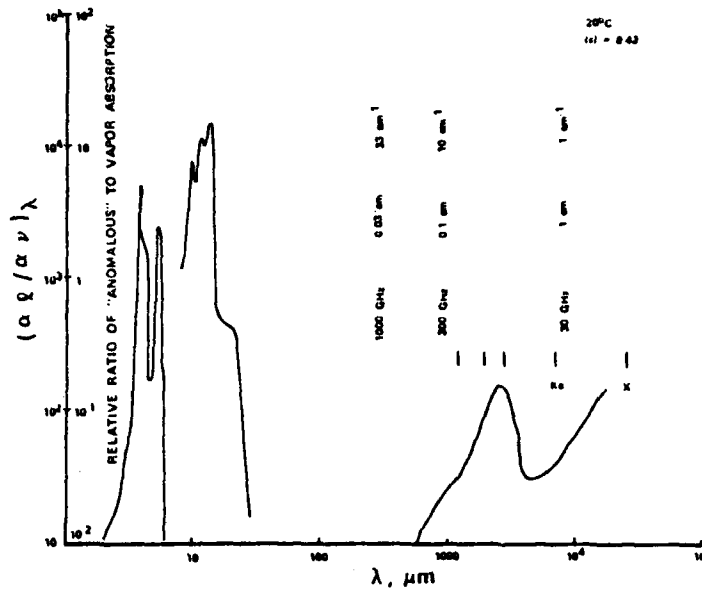


Figure 32. Ratio of Molecular Absorption Coefficients for Liquid Water and Water Vapor, vs. Wavelength.

e. "Because of changes in distributions of water vapor and ions with altitude in the earth's atmosphere, these cluster effects might influence global weather and climate in complex ways not previously understood." In the atmosphere, cosmic radiation produces many ions particularly at high altitudes. Mobility measurements of these ions<sup>41</sup> indicate that great numbers of them are hydrated ions or water ion clusters of mean size  $c_{\mu} = 10$  to 12 molecules. They could be represented by distributions like the lower curve in Figure 28. But, the profiles of atmospheric ion content, measured by electrical conductivity, versus altitude reveal many deviations from expected behavior. Interestingly, many of these deviations suggest that much larger fractions of water vapor may be clustered at higher altitudes than at sea level.<sup>70</sup> This would suggest that the spectroscopist on a mountain top might observe a larger anomalous absorption coefficient than would his counterpart at sea level. During a discussion with Professor L. C. Hale of The Ionosphere Research Laboratory, Pennsylvania State University, it was evidenced that this actually does occur not only in the infrared, but at longer (microwave) wavelengths as well. For example, a small absorption band near  $11.3 \mu\text{m}$ , which could be attributed to clusters, is found to be 2 to 3 times as intense in spectra taken at 3 km altitude as for similar spectra taken at sea level, as per a conversation with Dr. C. Gibbins of the Appleton Laboratory, Science Research Council, Slough, England. This concept is shown schematically in Figure 33. If the fraction of water vapor, which is clustered, does increase greatly with altitude, this finding would have a profound effect upon present models of atmospheric

radiation transfer. While water vapor (monomer) absorption is very small in the 8-13 $\mu$ m atmospheric window through which much of the earth's radiative transfer takes place, the cluster continuum absorption is intense. High concentrations of clusters at higher altitudes would form a very effective thermal "blanket" over the earth. The opacity of this thermal blanket would vary greatly with changes in temperature, saturation ratio, and ion-producing fluxes. One can think of ion-induced water cluster layers or "clouds", which differ from conventional clouds, in that the former are highly absorptive in the infrared but completely transparent in the visible wavelengths.<sup>24</sup>

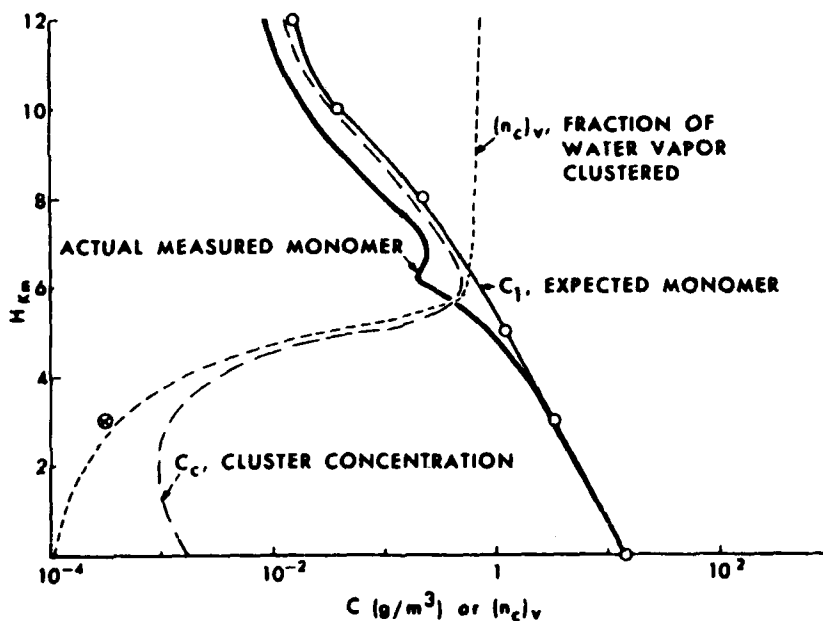


Figure 33. Schematic Representation of Possible Changes, with Altitude (H), km, in Water Cluster Concentration ( $C_c$ ) and Fraction of Vapor Clustered  $(n_c)_v$ , if the Extent of Clustering Were to Increase with Altitude Due to Cosmic Radiation. Also Shown Is the Expected Monomer Concentration ( $C_1$ ) from the U.S. Standard Atmosphere.

This concept of invisible clouds is perhaps easier to visualize when one realizes that substantial progress is being made in the detection of clear-air-turbulence (CAT) ahead of aircraft using infrared radiometers which monitor the water vapor "rotational band" near 20  $\mu$ m and at longer wavelengths.<sup>21</sup> This technology has advanced to the point where optimization of spectral passbands for most reliable detection is underway. It has been known for many years that turbulent atmospheric conditions are highly favorable to the formation of water

clusters or subvisible aerosols<sup>18</sup> which constantly change in a way which can modulate an infrared radiometer. CAT detection by a radiometer used to monitor these changes was first proposed by Carlon.<sup>20</sup> The same mechanisms are active in regions of CAT as are active in atmospheric clouds.

One could probably think of a conventional cloud as one happening to contain enough condensation nuclei to grow droplets large enough to be seen in the visible wavelengths by optical scattering. Water ion clusters or ion-induced neutral clusters also exist with droplets in normal clouds, or alone in regions of CAT. These clusters cannot grow to droplets because, in the absence of supersaturation (Figure 6), they cannot reach the critical cluster size for droplet nucleation. Their existence as equilibrium species in moist atmospheres is well known to cloud physicists.<sup>27</sup> Yet, because they do not grow large enough to scatter light, they may simply be assumed not to exist by atmospheric spectroscopists.

It is concluded that provocative evidence exists that ion, ion cluster, and ion-induced neutral water cluster behavior in the atmosphere is incompletely understood. The evidence suggests that cluster mechanisms may have important effects upon global weather and climate.

## 6. SUMMARY AND CONCLUSIONS

### 6.1 Summary.

The problem of infrared absorption by molecular clusters in water vapor has been investigated by parallel researches into four different aspects of the problem: (1) measurements of the infrared emission of steam and of steam-generated water vapor; (2) measurements of the electrical conductivity of moist air humidified by steam; (3) modeling of simple cluster configurations and comparison of theory with experimental data; and (4) a complete study of the thermodynamics of clustering up to the critical temperature of water. The results indicate that ions are important in the formation of ion hydrates or ion-induced, neutral water clusters which are found in great numbers in water vapor and moist air. Populations of these clusters are present in peaked distributions, probably with mean "sizes" of about 10 molecules per cluster. They exist independently of homogeneous clusters like the water dimer, which may also be significant in atmospheric processes. Cluster populations increase as the square of partial water vapor pressure, and their mean size decreases with increasing temperature, approaching unity (for hydrogen-bonded clusters) at the critical temperature, 374 °C. The clusters absorb infrared radiation (and apparently radiation at other wavelengths as well) due to modes of intermolecular or ion-molecule bonds. Their individual line spectra depend upon cluster configurations plus masses and bond strengths. The literature shows reasonable agreement between calculated and actual cluster absorption

wavelengths. Clustering in liquid water is much more extensive than in the vapor, but evidence exists that hydrogen bonds in clusters are similar to those in liquid water. Hence, that liquid data can be used for some cluster calculations. The hypothetical cluster formation and infrared absorption mechanisms cannot be directly verified experimentally, but there exists impressive evidence, based in part upon data from cloud chamber, radiometric and electrical conductivity measurements, that only certain mechanisms can explain all observations. It is concluded that anomalous absorption by water vapor, including the infrared continuum absorption, can be adequately explained by the presence of neutral or charged water clusters in the vapor phase.

## 6.2 Conclusions.

- The infrared continuum absorption of water "vapor" can be explained as the absorption due to intermolecular bonds in "liquidlike" clusters of water molecules which are present in fractions of about  $10^{-4}$  to  $10^{-3}$  in the vapor phase under typical ambient conditions.

- The water species responsible for the continuum absorption can be homogeneous, and limited to a few molecules (like the dimer). Or, their populations can have mean sizes of about 10 molecules and can be distributed in size from a few molecules to 30 or more. The latter kinds include ion clusters (ion hydrates) and ion-induced, neutral clusters.

- Cluster populations vary as the square of the water vapor partial pressure, and they decrease in mean size with increasing temperature or with decreasing saturation ratio (fractional, relative humidity). Thermodynamic consistency can be demonstrated in the behavior of clusters both in the vapor and liquid-phase from 0 °C to the critical temperature (374 °C), where these phases become one.

- The continuum absorption spectrum consists of lines contributed by modes of various bonds in clusters with differing configurations and populations which comprise the overall cluster population. Especially at higher temperatures (i.e., in steam), small bands appear in the spectrum which are spaced as predicted by simple intermolecular oscillator models. These bands can be observed by absorption or by emission and, in the latter case, frequently are associated with luminescencelike activity in warm water vapor.

- Measurements of the electrical conductivity of moist air show that the ion content increases very rapidly with temperature of vapor generation and that infrared absorption can, in fact, be accurately modeled as a function of the ion product of water with temperature. This allows the possibility

that, at least at higher temperatures, ion clusters or ion-induced, neutral clusters which have infrared absorption, can be generated by the dissociative ionization of water itself.

- The nature of cluster absorption should be resolvable in carefully-designed experiments to measure continuum absorption in a multi-pass optical cell, in the presence of an electrical field which can be varied with time and where the water vapor is generated at controlled temperatures and by different techniques.

- The anomalous spectral absorption of water vapor, which is called the "continuum absorption" in the infrared, apparently is not limited only to these shorter wavelengths. While a true continuum does not exist with increasing wavelength out to the microwave region, spectral intervals are found where absorption attributed to water clusters has been found. For example, the absorption near  $4 \text{ cm}^{-1}$  can be approximately as intense as the continuum absorption in the  $3\text{-}5 \mu\text{m}$  "window" region.

Commonality and close interrelationships exist between atmospheric water species described and measured by cloud physicists, investigators of electrical and electrostatic phenomena, and absorption or emission spectroscopists working in many wavelength regions. The numbers and kinds of cluster species can be described by techniques known to these disciplines. Provocative evidence exists which indicates that the extent of clustering may increase with altitude because of cosmic radiations. If so, a thermal "blanket" may exist for radiative transfer in the  $8\text{-}13 \mu\text{m}$  atmospheric "window" wavelength region whose opacity varies greatly with changes in temperature, saturation ratio, and ion-producing fluxes. This evidence suggests that water cluster mechanisms may have important effects upon global weather and climate.

### 6.3 Suggestions for Future Work.

- Vapor spectroscopists should give serious consideration to non-vapor cluster constituents of water in the atmosphere, including species which are ion-induced. Being smaller than critical size for nucleation of liquid water droplets, non-vapor cluster constituents of water in the atmosphere do not produce visible evidence of their presence, but are nevertheless capable of intense spectral activity, especially in the infrared.

- The entire water vapor spectrum, especially through the continuum absorption region and into the rotational band of water, should be carefully re-examined to determine which lines are best fitted by monomer models, and which lines are best described by water cluster models.

- Ion-induced cluster species should be considered in upper-atmospheric studies of the earth and perhaps in studies of other planetary atmospheres. Mass numbers of cluster species should be considered in the interpretation of all mass spectrometric data for all atmosphere samples.

- The nature of cluster absorption should be carefully resolved through experiments, for example, measuring the continuum absorption in a multi-pass cell, in the presence of an electrical field which can be varied with time and where water vapor is generated at controlled temperatures and by different techniques.

- Cluster activity should be suspected in considering atmospheric phenomena, which have no obvious explanation. Two examples are detection of CAT ahead of aircraft using far infrared radiometry, and the investigation of invisible plumes above chimneys carrying combustion gases to the atmosphere, wherein extremely high ion populations exist, as measured by electrical conductivity. Such plumes can persist for great distances from the chimneys which produced them.

- Further detailed studies should be conducted of the electrical conductivity and ion content of water vapor and moist air, particularly at elevated temperatures. The results may be important in the interpretation of theories of atmospheric, electrical, and electrostatic phenomena.

- Experiments should be conducted representing "marriages" of disciplines. For example, an infrared cloud chamber should be realizable, permitting studies of nucleation of subcritical clusters to be carried out without the need for droplet growth.

Faint, illegible text at the top of the page, possibly a header or introductory paragraph.

Second block of faint, illegible text, continuing the document's content.

**Blank**

Third block of faint, illegible text, appearing below the 'Blank' label.

#### LITERATURE CITED

1. Elsassser, W. M. NOTE ON ATMOSPHERIC ABSORPTION CAUSED BY THE ROTATIONAL WATER BAND. Phys. Rev. Vol. 53, p 768, (1938).
2. Goody, R. M. ATMOSPHERIC RADIATION I. THEORETICAL BASIS. Oxford: Clarendon Press, p 195-196, (1964).
3. Smith, R. A., Jones, F. E. and Chasmar, R. P. THE DETECTION AND MEASUREMENT OF INFRA-RED RADIATION. Oxford: Clarendon press, p 475, (1968).
4. Van Vleck, J. H. and Weiskopf, V. F. Reviews of Modern Physics Vol. 17, p 227, (1945).
5. Penner, S. S. QUANTITATIVE MOLECULAR SPECTROSCOPY AND GAS EMISSIVITIES. Reading, MA, Addison-Wesley Pub. Co. (1959).
6. Long, R. K., Mills, F. S. and Trusty, G. L. EXPERIMENTAL ABSORPTION COEFFICIENTS FOR ELEVEN CO LASER LINES. Report No. 3271-5, The Ohio State University Electroscience Laboratory 1973, UNCLASSIFIED.
7. Benedict, W. S. Canadian J. Phys. Vol. 34, p 847, (1951).
8. Varanasi, P., Chou, S. and Penner, S. S. "ABSORPTION COEFFICIENTS FOR WATER VAPOR IN THE 600-1000  $\text{cm}^{-1}$  REGION," J. Quant. Spectrosc. Radiat. Transfer 8, p 1537, (1968).
9. Burroughs, W. J., Jones, R. G. and Gebbie, H. A. "A STUDY OF SUBMILLIMETRE ATMOSPHERIC ABSORPTION USING THE HCN MASER", J. Quant. Spectrosc. Radiat. Transfer 9, 809.
10. Bignell, K. J. "THE WATER-VAPOR INFRA-RED CONTINUUM", Quart. J. Roy, Meteorol. Soc. Vol. 96, p 390, (1970).
11. Penner, S. S. "EFFECT OF DIMERIZATION ON THE TRANSMISSION OF WATER VAPOR IN THE NEAR-INFRARED", J. Quant. Spectrosc. Radiat. Transfer 13, p 383, (1973).
12. Gebbie, H. A., Emery, R. J., Bohlander, R. A. and Gimmetstad, G. G. Nature Vol. 247, p 456, (1974).
13. Emery, R. J., Moffat, P., Bohlander, R. A. and Gebbie, H. A. "MEASUREMENTS OF ANOMALOUS ATMOSPHERIC ABSORPTION IN THE WAVENUMBER RANGE 4  $\text{cm}^{-1}$  - 5  $\text{cm}^{-1}$ ", J. Atmos. and Terres. Phys. Vol. 37, p 587, (1975).

14. Gimmestad, G. G. and Gebbie, H. A. "ATMOSPHERIC ABSORPTION IN THE RANGE 12  $\text{cm}^{-1}$  - 32  $\text{cm}^{-1}$  MEASURED IN A HORIZONTAL PATH", J. Atmos. and Terres. Phys. Vol. 38, p 325, (1976).
15. Curtiss, L. A. and Pople, J. A. "AB INITIO CALCULATION OF THE BIRATIONAL FORCE FIELD OF HTE WATER DIMER", J. Molec. Spectrosc. Vol. 55, p 1, (1975).
16. Owicki, J. C., Shipman, L. L. and Scheraga, H. A. "STRUCTURE, ENERGETICS AND DYNAMIC OF SMALL WATER CLUSTERS", J. Phys. Chem. Vol. 79, p 1794, (1975).
17. Inter-Union Commission on Radio-Meteorology; Paper presented at the Colloquium on Probing of Atmospheric Constituents, Bournemouth, England, 14-21 May 1975.
18. Carlon, H. R. "THE APPARENT DEPENDENCE OF TERRESTRIAL SCINTILLATION INTENSITY UPON ATMOSPHERIC HUMIDITY", Applied Optics Vol. 4, p 1089-1097, (1965).
19. Bryan, J. B. and Curnutte, B. "A NORMAL COORDINATE ANALYSIS BASED ON THE LOCAL STRUCTURE OF LIQUID WATER", J. Molec. Spectroscopy vol. 41, p 512, (1972); also see Curnutte, B. and Bandekar, J., "THE INTRAMOLECULAR VIBRATIONS OF THE WATER MOLECULE IN THE LIQUID STATE", J. Molec. Spectroscopy Vol. 41, p 500, (1972).
20. Carlon, H. R. "HUMIDITY EFFECTS IN THE 8-13  $\mu\text{m}$  INFRARED WINDOW", Applied Optics Vol. 5, p 879, (1966).
21. Kuhn, P. M., Nolt, I. G. and Stearns, L. P. INFRARED PASSBANDS FOR CLEAR-AIR-TURBULENCE DETECTION. J. V. Radostitz, co-author. Optics Letters Vol. 3, p 130, (1978).
22. Streete, J. L. "INFRARED MEASUREMENTS OF ATMOSPHERIC TRANSMISSION AT SEA LEVEL", Applied Optics Vol. 7, p 1545, (1968).
23. Carlon, H. R. "INFRARED EMISSIONS BY FINE WATER AEROSOLS AND FOGS", Applied Optics Vol. 9, p 2000-2006, (1970).
24. Carlon, H. R. "MODEL FOR INFRARED EMISSION OF WATER VAPOR/AEROSOL MIXTURES", Applied Optics Vol. 10, p 2297, (1971).
25. Hodges, J. A. "AEROSOL EXTINCTION CONTRIBUTION TO ATMOSPHERIC ATTENUATION IN INFRARED WAVELENGTHS", Applied Optics Vol. 11, p 2304.
26. Carlon, H. R., Anderson, D. H., Milham, M. E., Tarnove, T. L., Frickel, R. H. and Sindoni, I. "INFRARED EXTINCTION SPECTRA OF SOME COMMON LIQUID AEROSOLS", Applied Optics Vol. 16, p 1598, (1977).

27. Wilson, J. G. "THE PRINCIPLES OF CLOUD CHAMBER TECHNIQUE", Cambridge Monographs on Physics. University Press, Cambridge, England, (1951).
28. Hale, B. N. and Plummer, P. L. M. "ON NUCLEATION PHENOMENA I: A MOLECULAR MODEL", J. Atmos. Sci. Vol. 31, p 1615, (1974).
29. Potter, W. R. and Hoffman, J. G. "PHASE TRANSITION LUMINESCENCE IN BOILING WATER; EVIDENCE FOR CLUSTERS", Infrared Physics Vol. 8, p 265, (1968).
30. Wolynes, P. G. and Roberts, R. E. "MOLECULAR INTERPRETATION OF THE INFRARED WATER VAPOR CONTINUUM", Applied Optics Vol. 17, p 1484, (1978).
31. Carlon, H. R. "MOLECULAR INTERPRETATION OF THE IR WATER VAPOR CONTINUUM: COMMENTS", Applied Optics Vol. 17, p 3193, (1978).
32. Carlon, H. R. "PHASE TRANSITION CHANGES IN THE MOLECULAR ABSORPTION COEFFICIENT OF WATER IN THE INFRARED: EVIDENCE FOR CLUSTERS", Applied Optics Vol. 17, p 3192, (1978).
33. Roberts, R. E., Selby, J. E. A. and Biberman, L. M. "INFRARED CONTINUUM ABSORPTION BY ATMOSPHERIC WATER VAPOR IN THE 8-12  $\mu\text{m}$  WINDOW", Applied Optics Vol. 15, p 2085, (1976).
34. Carlon, H. R. ANOMALOUS INFRARED EMISSION FROM CONDENSING AND COOLING STEAM CLOUDS, ARCSL-TR-78001, Chemical Systems Laboratory (ADA 050 083), Aberdeen Proving Ground, MD 21010, December 1977, UNCLASSIFIED.
35. Carlon, H. R., Milham, M. E. and Frickel, R. H. "DETERMINATION OF AEROSOL DROPLET SIZE AND CONCENTRATION FROM SIMPLE TRANSMITTANCE MEASUREMENTS", Applied Optics Vol. 15, p 2454, (1976).
36. Castleman, Jr., A. W. "NUCLEATION PROCESS AND AEROSOL CHEMISTRY", Space Sci. Rev. Vol. 15, p 547, (1974).
37. Newton, M. D. "AB INITIO STUDIES OF THE HYDRATED  $\text{H}_3\text{O}^+$  ION II. THE ENERGETICS OF PROTON MOTION IN HIGHER HYDRATES ( $n = 3-5$ )", J. Chem. Phys. Vol. 67(12), p 5535, (1977).
38. Searcy, J. Q. and Fenn, J. B. "CLUSTERING OF WATER ON HYDRATED PROTONS IN A SUPERSONIC FREE JET EXPANSION", J. Chem. Phys. Vol. 61, p 5282, (1974).
39. Castleman, Jr., A. W., Holland, P. M. and Keesee, R. G. "THE PROPERTIES OF ION CLUSTERS AND THEIR RELATIONSHIP TO HETEROMOLECULAR NUCLEATION", J. Chem. Phys. Vol. 68, p 1760-1767, (1978).

40. Wright, H. L. Proc. Phys. Soc. London Vol. 48, p 675, (1936).
41. Chalmers, J. A. ATMOSPHERIC ELECTRICITY, Pergammon Press, p 86-88, (1967).
42. Gerdien, H. Phys. Z. Vol. 6, p 800, (1905).
43. Holzapfel, W. J. Chem. Phys. 50, 4424, as discussed by F. Franks, ed. WATER: A COMPREHENSIVE TREATISE. VOL. 1. Plenum Press, New York, NY p 503-504, (1969).
44. Curnutte, B. and Bandekar, J. "INTRAMOLECULAR VIBRATIONS OF THE WATER MOLECULE IN THE LIQUID STATE", J. Molec. Spectrosc. Vol. 41, p 500, (1972).
45. Carlon, H. R. INTRODUCTION TO POLYMOLECULAR WATER CLUSTERS AND THEIR INFRARED ACTIVITY, ARSCL-TR-78014, (ADA 052 699), Chemical Systems Laboratory, Aberdeen Proving Ground, MD 21010, 1978, UNCLASSIFIED.
46. Carlon, H. R. A MOLECULAR-CLUSTER (ION HYDRATE) EXPLANATION OF THE INFRARED WATER VAPOR CONTINUUM ABSORPTION, ARSCL-TM-78001, Chemical Systems Laboratory, Aberdeen Proving Ground, MD 21010, August 1978.
47. Carlon, H. R. INFRARED ABSORPTION BY WATER CLUSTERS, Invited seminar presented at the Graduate Center for Cloud Physics Research, University of Missouri, Rolla, MO 65401, 1978.
48. Israel, H. ATMOSPHERIC ELECTRICITY. VOL. 1. Israel Program for Scientific Translations at Jerusalem, 1971.
49. Castleman, Jr., A. W. and Tang, I. N. "ROLE OF SMALL CLUSTERS IN NUCLEATION ABOUT IONS", J. Chem. Phys. Vol. 57, p 3629, (1972).
50. Carlon, H. R. VARIATIONS IN EMISSION SPECTRA FROM WARM WATER FOGS: EVIDENCE FOR CLUSTERS IN THE VAPOR PHASE, ARSCL-TM-78002, Chemical Systems Laboratory, Aberdeen Proving Ground, MD 21010, August 1978.
51. Carlon, H. R.; 1979a. VARIATIONS IN EMISSION SPECTRA FROM WARM WATER FOGS: EVIDENCE FOR CLUSTERS IN THE VAPOR PHASE. Accepted for Infrared Physics, January 1979, 1-16.
52. Hale, G. M. and Querry, M. R. "OPTICAL CONSTANTS OF WATER IN THE 200-nm TO 200-mu WAVELENGTH REGION", Applied Optics Vol. 12, p 555, (1973).

53. Falk, M. and Gigurere, P. A. "INFRARED SPECTRUM OF THE  $H_3O^+$  ION IN AQUEOUS SOLUTIONS", Canadian J. Chem. Vol. 35, p 1195, (1957).

54. Frank, H. S., "Water: A Comprehensive Treatise", Structural Models, Vol. 1, Olenum Press, New York, NY, 1972.

55. Frank, H. S. and Wen, W. Y. "STRUCTURAL ASPECTS OF ION-SOLVENT INTERACTION IN AQUEOUS SOLUTION: A SUGGESTED PICTURE OF WATER STRUCTURE", Disc. Faraday Soc. Vol. 24, p 133, (1957).

56. Pinkley, L. W., Sethna, P. P. and Williams, D. "OPTICAL CONSTANTS OF WATER IN THE INFRARED; INFLUENCE OF TEMPERATURE", J. Opt. Soc. Amer. Vol. 67, p 494, (1977).

57. W. A. P. Luck as discussed by Walrafen, G. E. WATER: A COMPREHENSIVE TREATISE. F. Franks, ed. (Vol. 1) Plenum Press, New York, NY, p 210.

58. Mie, G. Ann. Physik Vol. 25, p 377, (1908).

59. Wolfe, W. L., ed. HANDBOOK OF MILITARY INFRARED TECHNOLOGY. US Office of Naval Research, Dept. of the Navy, at Washington, DC, 1965.

60. Carlon, H. R. ELECTRICAL CONDUCTIVITY OF MOIST AIR I: CELL DESIGN AND FABRICATION FROM THE WATER CLUSTER THEORY. ARCSL-TR-78007, (ADA 056 235), Chemical Systems Laboratory, Aberdeen Proving Ground, MD 21010, 1978, UNCLASSIFIED.

61. Carlon, H. R. INFRARED ABSORPTION BY WATER CLUSTERS: FINAL REPORT. ARCSL-TR-79013, Chemical Systems Laboratory, Aberdeen Proving Ground, MD 21010, January 1979.

62. Carlon, H. R. 1979e. "ION CONTENT OF AIR HUMIDIFIED BY BOILING WATER", J. of Appl. Phys. Vol. 51, p 171-173, (1980).

63. Blanchard, D. C. THE ELECTRIFICATION OF THE ATMOSPHERE BY PARTICLES FROM BUBBLES IN THE SEA. Woods Hole Oceanographic Institute, Reference 61-9, 1961.

64. Moore, A. D., ed. "ELECTROSTATICS AND ITS APPLICATIONS", Wiley & Sons, New York, NY p 390, 1973.

65. McDonald, J. E. "HOMOGENEOUS NUCLEATION OF VAPOR CONDENSATION I. THERMODYNAMIC ASPECTS", Amer. J. Phys. Vol. 30, p 870, (1962).

66. McDonald, J. E. "HOMOGENEOUS NUCLEATION OF VAPOR CONDENSATION II. KINETIC ASPECTS", Amer. J. Phys. Vol. 31, p 31, (1963).

67. Abraham, F. F. HOMOGENEOUS NUCLEATION THEORY.  
Academic Press, New York (1974).

68. Montgomery, Jr., G. P. "TEMPERATURE DEPENDENCE OF  
INFRARED ABSORPTION BY THE WATER VAPOR CONTINUUM NEAR 1200  
cm<sup>-1</sup>", Applied Optics Vol. 17, p 2299, (1978).

69. Wilson, C. T. R. Philos. Trans. Vol. 189, p 265,  
(1897).

70. Wilson, C. T. R. Philos. Trans. Vol. 192, p 403,  
(1899).

**LMED**  
**8**